Beneficial effects of the AT_2 receptor agonist buloxibutid (C21) against acute alveolar epithelial cell inflammation during anti-viral responses

Authors: Franco Conforti[1,2], Joseph Bell[1,2], Robert Ridley[1,2], Lareb Dean[1,2], Matthew Loxham[1,2], James Parkin[1,2], Aiman Alzetani[2,3], Mark G Jones[1,2], Carl-Johan Dalsgaard[4], Johan Raud[4] and Donna E Davies[1,2].

Affiliations:
[1]Clinical and Experimental Sciences, Faculty of Medicine, University of Southampton, Southampton SO16 6YD, UK.
[2]NIHR Southampton Biomedical Research Centre, University Hospital Southampton, Southampton SO16 6YD, UK;
[3]University Hospital Southampton, Southampton SO16 6YD, UK;
[4]Vicore Pharma AB, Stockholm, Sweden.

Correspondence: Franco Conforti, Clinical and Experimental Sciences, Faculty of Medicine, University of Southampton, Southampton SO16 6YD, UK. E-mail: fc3g11@soton.ac.uk.

Take-home message:

- The potent AT_2 receptor agonist, buloxibutid, reduces the proinflammatory pathogenetic response in a model of viral infection in primary human ATII cells.
- Crucially, buloxibutid treatment does not alter the protective alveolar antiviral responses.

Conflict of interest: JR is an employee of Vicore Pharma AB and holds shares and share options in the company. C-JD is a former employee of Vicore Pharma AB and holds shares and share options in the company. FC, JB, RR, LD, ML, JP, AA, MGJ and DD have nothing to declare.

ABSTRACT

Aim: Activation of the angiotensin II type 2 receptor (AT_2 receptor; encoded by *AGTR2*) has been shown to be beneficial during tissue injury and repair. Therefore, we aimed to investigate the expression of AT_2 receptor in human alveolar type II (ATII) cells, a cell population responsible of lung repair and regeneration and the effect of the AT_2 receptor agonist buloxibutid (also known as C21), in an *in vitro* model of viral infection using primary ATII cells.

Methods: We described the expression of AT_2 receptor mRNA using publicly available lung single-cell RNA sequencing datasets. We evaluated the effects of buloxibutid on ATII cell biology at baseline and in response to treatment with double stranded RNA (polyinosinic:polycytidylic acid, a pathogen associated molecular pattern) using MTS cytotoxicity assay, transcriptomic analysis and ELISA.

Results: We found that buloxibutid was well tolerated by ATII cells under all conditions tested. RNA sequencing demonstrated that ATII cells responded to polyinosinic:polycytidylic acid with induction of a characteristic antiviral innate immune response. Gene set enrichment analysis revealed that buloxibutid caused a significant suppression of polyinosinic:polycytidylic acid-induced pro-inflammatory

responses whereas it was without effect on the expression of antiviral genes.

Conclusions: Our findings suggest that buloxibutid may have therapeutic potential for treatment of respiratory viral pneumonias by limiting excessive pro-inflammatory responses that have the potential to lead to a cytokine storm, while maintaining a protective antiviral response.

INTRODUCTION

The renin-angiotensin system (RAS) is an important hormonal system that plays a crucial role not only in regulating blood pressure and fluid balance in the body but also in the pathophysiology of several diseases affecting the kidney, neuronal system, cardiocirculatory system and lung. The Angiotensin II (Ang-II) hormone is the principal mediator of the RAS acting via the angiotensin II type 1 receptor (AT_1 receptor), which is abundantly expressed in different tissues, and the angiotensin II type 2 receptor (AT_2 receptor), the expression of which has been shown to increase during tissue injury. Pharmacological activation of the AT_2 receptor has shown significant therapeutic benefit, as well as an ability to modulate immune and stem cell responses in order to promote tissue repair and regeneration (Fatima, Patel and Hussain 2021).

Circulating angiotensin I (Ang-I) is cleaved to generate angiotensin II (Ang-II) through the activity of angiotensin converting enzyme (ACE). Ang-II acts on AT_1 receptor or AT_2 receptor with opposing effects: AT_1 receptor promotes inflammation, fibrosis, alveolar-endothelial damage and increases microvascular permeability, while AT_2 receptor reduces inflammation, promotes alveolar-endothelial survival together with barrier integrity, and can reduce oedema and lung fibrosis (Wang et al. 2019). ACE is abundantly expressed in the

pulmonary capillary network and so, in some pathological conditions, Ang-II can cause excessive activation of AT_1 receptor to cause increased alveolar-capillary permeability, alveolar oedema, hypoxemia, sepsis and possibly death (Wang et al. 2019, Patel et al. 2020).

Since the availability of the non-peptide AT_2 receptor agonist buloxibutid, the anti-inflammatory effect of AT_2 receptor activation has been validated in different models of tissue injury and disease including brain injury, atherosclerosis, arthritis and kidney injury (Gao et al. 2022, Jabber, Mohammed and Hadi 2023, Sampson et al. 2016, Ismael and Ishrat 2022, Steckelings et al. 2022). In murine models of acute and chronic cigarette smoke-induced chronic obstructive pulmonary disease, activation of the AT_2 receptor by buloxibutid has been reported to exhibit anti-inflammatory effects resulting in the restoration of the lung function (Mei et al. 2020). However, little is known about the effects of buloxibutid in injury/repair of the human lung when homeostasis is perturbated by a viral infection. In cases of viral pneumonia, alveolar epithelial cells and vascular endothelial cells are damaged leading to the abnormal accumulation of fluid in the lung alveoli. This is accompanied by release of inflammatory cytokines from both immune and non-immune cells. If the inflammatory response is excessive, acute lung injury (ALI) or even acute respiratory distress syndrome (ARDS) can develop (Gao et al. 2020). The recent COVID-19 pandemic has

increased awareness of the potential deadly consequences of severe viral pneumonia caused by viruses like SARS-CoV-2, respiratory syncytial virus (RSV) as well as influenza and has highlighted the need for better control of virus-induced inflammation.

Considering the critical role of RAS homeostasis in lung injury and repair, we postulated that the AT_2 receptor agonist buloxibutid would control inflammatory responses in primary human ATII cells exposed to polyinosinic:polycytidylic acid (poly I:C), a synthetic double-stranded RNA which was used to mimic a viral infection.

RESULTS

Buloxibutid treatment did not show any significant cytotoxicity on primary human ATII cells.

Buloxibutid is a potent agonist of AT_2 receptor and its activation has been reported to be beneficial in different lung conditions where ATII cells play a vital role in lung homeostasis (Mei et al. 2020, Menk et al. 2018, Sumners et al. 2019, Steckelings and Sumners 2020). Data mining of online published single cell-sequencing datasets (Habermann et al. 2020, Sikkema et al. 2023) of normal and pathological lung tissue identified that AT_2 receptor is mainly expressed in ATII cells (Fig.1A and Supp.

Fig.1) thus identifying these cells as a likely therapeutic target. In our dose response experiments, exposure of primary human ATII cells to buloxibutid in absence or presence of poly I:C did not affect cell morphology or cell density (Supp. Fig.2). Similarly, using an MTS cytotoxicity assay, we found no significant harmful effects of buloxibutid on primary human ATII cells in presence or absence of poly I:C (Fig.1B). Moreover, buloxibutid treatment did not affect AT_2 receptor gene (*AGTR2*) expression in ATII cells (Fig.1C). Our findings strongly suggest that buloxibutid is well tolerated by ATII cells and does not negatively regulate AT_2 receptor gene expression.

Buloxibutid treatment inhibits inflammatory cytokine release in response to poly I:C without modulating antiviral genes.

Polyinosinic:polycytidylic acid (poly I:C) is a synthetic analogue of double-stranded (ds)RNA that mimics viral infection by activating the RNA viral sensors, Toll-like receptor 3 (TLR3) and RNA helicases (Harris et al. 2013). Therefore, for initial experiments, we performed a dose-response study by treating ATII cells with different concentrations of buloxibutid in absence or presence of poly I:C. Consistent with the anti-inflammatory role of AT_2 receptor, we found that a small, non-significant suppressive effect of Buloxibutid on polyI:C-induced IL-6 gene

expression (p=0.99, 0.73, 0.27 for 1000 nM buloxibutid vs control, 10nM, and 100 nM buloxibutid, respectively) was accompanied by a significant decrease in IL-6 protein release (Fig.2A). In contrast, the ability of double stranded RNA to induce *MX1* and *RSAD2*, interferon-inducible genes that inhibit the replication of a variety of viruses including HIV and influenza (Schoggins and Rice 2011), was not affected by buloxibutid treatment (Fig.2B). Our findings suggest a distinct anti-inflammatory role for buloxibutid during viral infection while maintaining antiviral gene expression.

RNA-sequencing show a significant effect of buloxibutid treatment on inflammatory pathways without affecting antiviral responses.

In order to further evaluate the anti-inflammatory role of buloxibutid in the context of a viral infection, we performed RNA-sequencing on ATII cells treated without and with buloxibutid in presence or absence of poly I:C. Bioinformatic analysis showed that gene expression profiles were largely dependent on presence or absence of poly I:C (Fig.3A), where the top differentially expressed genes were identified as being involved in cellular response to virus (Fig.3B).

Virus infection activates specific proinflammatory pathways that include the interferon system, JAK-STAT and NF-κB which in turn promote the expression of cytokines, chemokines and anti-viral factors in order to preserve tissue homeostasis and block viral spreading (Nan, Wu and Zhang 2017, Pfeffer 2011). In order to understand how changes in the expression of individual genes might reflect broader changes within the cell, we performed gene set enrichment analysis, which highlights pathways enriched in differentially expressed genes in our RNA-seq results. This showed that, in the presence of polyI:C, buloxibutid significantly downregulated a range of inflammation-associated pathways (Fig.4A). Further interrogation of these pathways individually showed that the effect of buloxibutid was seen across multiple genes within each pathway, and cells were clearly defined by the presence or absence of buloxibutid (Fig.4B and Supp. Table2). Of note, some of the pro-inflammatory factors and chemokines down-regulated by buloxibutid (Fig.5A and Supp. Fig.3) are those that have been implicated as mediators of the cytokine storm, a hyperinflammatory state that is associated with severe uncontrolled respiratory viral infection in some individuals (Murdaca et al. 2021, Kirsch-Volders and Fenech 2021). In contrast key antiviral transcripts were not affected by buloxibutid treatment (Fig.5B). These findings demonstrate the potential of buloxibutid to act exclusively as an anti-inflammatory agent with

no effect on the antiviral cell response during a respiratory viral infection.

Discussion and conclusions

Our work provides evidence of an anti-inflammatory effect of the AT_2 receptor agonist buloxibutid in our model of viral infection in primary human ATII cells. Buloxibutid was able to significantly attenuate inflammation pathways including markers of acute inflammation that are typical of the deleterious cytokine storm. Most importantly, the advantageous anti-inflammatory effect of buloxibutid did not alter the crucial alveolar antiviral responses that are required to control viral replication and spread and so limit further progression of virus-induced lung injury.

The global impact in human history of respiratory diseases like Spanish flu, SARS, MERS, influenza A H1N1 2009 and COVID-19 highlight the crucial role of proinflammatory pathogenetic mechanisms in the respiratory system known as “cytokine storm”. During a respiratory viral infection, a normal immune response to tackle virus spreading can progress in an uncontrolled immune response characterised by an hyperinflammatory status typical of the so called cytokine storm (Murdaca et al. 2021, Kirsch-Volders and Fenech 2021). As respiratory viruses develop various strategies to evade the anti-

viral immune response the rapidly growing infection triggers the uncontrolled production of typical mediators of the cytokine storm including cytokines such as IL-6, IL-8, IL-1β and GM-CSF, and chemokines such as CCL2, CCL-5, IP-10 and CCL3. This is due an exaggerated activation and expansion of immune cells leading to hypersecretion of deleterious amounts of proinflammatory cytokines resulting in acute lung damage, systemic inflammation, multiorgan dysfunction and possibly death (Murdaca et al. 2021, Kirsch-Volders and Fenech 2021). During the COVID19 pandemic, many people died due to the cytokine storm induced by SARS-CoV2 due to the limited availability of effective anti-inflammatory therapy for COVID-19. Corticosteroids such as dexamethasone were widely used after platform trials demonstrated a significant decrease in mortality among patients who were receiving either invasive mechanical ventilation or oxygen alone at randomization but not among those receiving no respiratory support (Group et al. 2021). While corticosteroids have a potent anti-inflammatory effect, they also suppress the antiviral response (Bahsoun et al. 2023). In fact recent studies have indicated increased mortality and delayed viral clearance when either high dose corticosteroids or early initiation of treatment was administered (Cron 2022, Bahsoun et al. 2023). In contrast to corticosteroids, buloxibutid is able to reduce inflammation while retaining the protective antiviral response. Moreover, buloxibutid has shown efficacy in COVID-

19 caused by the original Wild-Type SARS-CoV-2 variant that replicates primarily in ATII cells (Tornling et al. 2021, Szekely et al. 2021). In this study, treatment of hospitalised patients with moderately severe COVID-19 with buloxibutid for 7 days on top of standard of care (including glucocorticoids and remdesivir in the majority of the subjects) reduced the requirement for oxygen supplementation.

In view of the critical role of proinflammatory pathogenetic mechanisms involved in severe lung viral infections, there is a strong need to identify the most suitable immunomodulatory strategy that does not blunt the antiviral response. Our results suggest that buloxibutid could be a potential approach to dampen the pathogenetic cytokine storm while leaving the antiviral mechanism unaltered in order to suppress residual virus spread and limit further tissue damage. Most importantly, by acting upstream of the cytokine storm network, buloxibutid could help to prevent damage to alveolar epithelium and of the microvasculature, modulating the exaggerated infiltration of inflammatory cells and promoting epithelial repair (Fig.6). While this study provides important insights into the cellular responses of alveolar epithelial cells during viral mimic stimulation, certain limitations should be acknowledged. First, all experiments were conducted in vitro, which, while allowing for controlled mechanistic investigations, may not fully capture the complex interactions present in the in vivo lung environment, including cell

crosstalk, vascular influences, and effects of the tissue microenvironment. Second, although the use of primary cells is a strength of this study, the relatively small number of experimental replicates (n) and donors is a limitation. Third, although ATII cells are a key component of the distal lung and play a central role in respiratory viral infections, we did not assess responses in airway epithelial cells, which represent the initial site of viral entry and are crucial in early response to viral infection. Lastly, we used polyI:C as a surrogate for viral infection. While polyI:C is a well-established tool to study innate immune activation, it does not fully replicate the complexities of live viral infection, including viral replication and shedding. Future studies incorporating live virus models would be valuable to confirm the relevance of our findings.

METHODS

Primary alveolar type II (ATII) isolation

Human lung experiments were approved by the Southampton and South-West Hampshire and the Mid and South Buckinghamshire Local Research Ethics Committees, and all subjects gave written informed consent.

Primary ATII culture were established from macroscopically normal regions of surgically resected lung parenchyma tissue in

accord with the method described by Witherden et al. ,2001(Witherden and Tetley 2001). Briefly, the lung tissue was perfused with 0.9% sodium chloride solution and infused with 0.25% Trypsin solution (Sigma-Aldrich, Poole, UK) at 37 °C for 45 min. After trypsin digestion, the tissues were finely cut in the presence of newborn calf serum (NCS) (Life Technologies Limited, Paisley, UK) and DNase 250 µg/ml (Sigma-Aldrich, Poole, UK), then cells were filtered by sequential passage through a 400-µm metal mesh and 40- µm nylon filter. The cells were re-suspended in DCCM-1 medium (Biological Industries Ltd, Kibbutz Beit-Haemek, Israel) supplemented with 1% penicillin, 1% streptomycin, and 1% L-glutamine, and incubated at 37 °C in a humidified incubator for 2 h in tissue culture flasks to allow differential adherence and removal of contaminating cells. The ATII cells were re-suspended in fresh DCCM-1 supplemented with 10% NCS, 1% penicillin, 1% streptomycin and 1% L-glutamine (all supplememts from Life Technologies Limited, Paisley, UK) and plated on collagen 1 (PureCol 5005-b, Advanced BioMatrix Inc, California, USA) coated 96-well plates at 60% density; after 48h purity was tested by staining for alkaline phosphatase.

Cell treatment and cytoxicity assay

Buloxibutid was dissolved in dimethylsulphoxide (DMSO) (Sigma-Aldrich, Gillingham, UK) at a final concentration of 0.1% and 0.1% DMSO was used as vehicle CTRL. Human primary ATII cells at passage 1 were cultured at a cell density of 70-80% on collagen 1 (PureCol 5005-b, Advanced BioMatrix Inc, California, USA) coated 96well plate and treated for 24h without or with buloxibutid in presence or absence of poly I:C HMW (InvivoGen Europe, Toulouse, France). After 24h treatment, any cytotoxic effect has been evaluated using an MTS assay *CellTiter 96® AQ$_{ueous}$ One Solution Cell Proliferation Assay* from Promega UK Ltd. in accord with the manufacture instruction. A vehicle control (DMSO) was run in each experiment.

Reverse transcription and quantitative PCR (RTqPCR)

Human primary ATII cells were cultured at a cell density of 70-80% on collagen 1 coated 96 well plate and treated for 24h without or with buloxibutid in presence or absence of poly I:C (InvivoGen Europe, Toulouse, France). After the 24h treatment, RNA was isolated using Monarch® Total RNA Miniprep Kit (New England Biolabs Limited, Herts, UK). RNA was reversed to cDNA using precision nanoScript2 Reverse Transcription Kit from Primer Design, Southampton, UK or High-Capacity cDNA Reverse Transcription Kit from Life Technologies Limited, Paisley, UK.

Probe-based qPCR primers sets were obtained from Primer Design, Southampton, UK (*MX1 catalog no. DD-hu-600-MX1; RSAD2 catalog no. DD-hu-600-RSAD2; UBC/GAPDH catalog no. HK-PP-hu-d-UBC/GAPDH)* and SYBR green qPCR primers sets were obtained from Life Technologies Limited, Paisley, UK (*IL6: FW-CTGGCAACAATGAGTCTACCTT and RV-GCCACAGCGAGGTTGAAGAT; AGTR2: FW-ACTCACCTCTTCAGAACGAATTG and RV-CCATCTTTGGAAGGTTCAGGTTG).* Changes in mRNA expression using the following primers were analysed by qPCR and normalized to the housekeeping genes ubiquitin C and glyceraldehyde-3-phosphate dehydrogenase *(UBC* and GAPDH*)*. Data were analysed using the ΔΔCT method.

ELISA and multiplex electrochemiluminescence immunoassay analysis

Human Interleukin 6 (IL6) and Monocyte chemoattractant protein-1 (MCP1) were evaluated in culture media using a DuoSet ELISA (R&D, Abingdon, UK) in accordance with manufacturer's instructions. Human Interleukin 15 (IL15), Human Interleukin 1-beta (IL1β), Macrophage Inflammatory Protein 1 Alpha (MIP1a) and tumor necrosis factor alpha (TNFα) were evaluated in culture media using a multiplex electrochemiluminescence immunoassay (U-PLEX MSD, Rockville, Maryland, USA). Each sample was evaluated in

duplicates and the mean value used for subsequent analyses. $p<0.05$ was accepted as statistically significant. * $p<0.05$.

RNA sequencing and Bioinformatic Analyses

Cells were harvested 24h after treatment and RNA was isolated using Monarch® Total RNA Miniprep Kit (New England Biolabs). RNA sequencing was performed by Novogene (UK) using an Illumina Novaseq 6000 sequencer after passing the quality control checks. RNA samples were enriched for mRNA using polyA enrichment using poly-T-oligo magnetic beads. After fragmentation, cDNA was synthesised using random hexamer primers. ~150bp paired end read sequencing was performed on an Illumina Novaseq 6000 sequencer. Kallisto running in paired-end mode was used to pseudoalign raw fastq data with human reference transcriptome hg38 (from human reference genome GRCh38), using RefSeq's transcripts to generate raw counts data. Raw counts were imported into R using the tximport package. Differential expression analysis was performed using edgeR, with Benjamini-Hochberg multiple test correction. Normalised counts per million reads (CPM) were calculated using EdgeR. Gene set enrichment analysis was performed using NCBI's GSEA software (https://www.gsea-msigdb.org/gsea/index.jsp), run in preranked mode, with genes ranked by -log10 (adjusted P-value). Heatmaps were produced using pheatmap. Graphs were produced using ggplot2.

Statistics

All the experiments were performed using 4 different donors (3 male and 1 female) . ‘n’ indicates the number of repeated experiments with different donors. ELISA and qPCR results are expressed as means of ± SD. Differences between groups were assessed using Kolmogorov-Smirnov test, Mann-Whitney test, oneway-ANOVA or 2ways-ANOVA test with Dunnett’s multiple comparisons test. All data were analysed using Prism (GraphPad, CA, USA). $p<0.05$ was accepted as statistically significant. * $p<0.05$ and p-value < 0.01 **.

References

Bahsoun, A., Y. Fakih, R. Zareef, F. Bitar & M. Arabi (2023) Corticosteroids in COVID-19: pros and cons. *Front Med (Lausanne),* 10**,** 1202504.

Cron, R. Q. (2022) No perfect therapy for the imperfect COVID-19 cytokine storm. *Lancet Rheumatol,* 4**,** e308-e310.

Fatima, N., S. N. Patel & T. Hussain (2021) Angiotensin II Type 2 Receptor: A Target for Protection Against Hypertension, Metabolic Dysfunction, and Organ Remodeling. *Hypertension,* 77**,** 1845-1856.

Gao, W., L. Shen, D. D. Long, T. T. Pan, D. Wang, X. Q. Chai & S. S. Hu (2022) Angiotensin II type 2 receptor pharmacological agonist, C21, reduces the inflammation and pain hypersensitivity in mice with joint inflammatory pain. *Int Immunopharmacol,* 110**,** 108921.

Gao, Y. L., Y. Du, C. Zhang, C. Cheng, H. Y. Yang, Y. F. Jin, G. C. Duan & S. Y. Chen (2020) Role of Renin-Angiotensin System in Acute Lung Injury Caused by Viral Infection. *Infect Drug Resist,* 13**,** 3715-3725.

Group, R. C., P. Horby, W. S. Lim, J. R. Emberson, M. Mafham, J. L. Bell, L. Linsell, N. Staplin, C. Brightling, A. Ustianowski, E. Elmahi, B. Prudon, C. Green, T. Felton, D. Chadwick, K.

Rege, C. Fegan, L. C. Chappell, S. N. Faust, T. Jaki, K. Jeffery, A. Montgomery, K. Rowan, E. Juszczak, J. K. Baillie, R. Haynes & M. J. Landray (2021) Dexamethasone in Hospitalized Patients with Covid-19. *N Engl J Med,* 384**,** 693-704.

Habermann, A. C., A. J. Gutierrez, L. T. Bui, S. L. Yahn, N. I. Winters, C. L. Calvi, L. Peter, M. I. Chung, C. J. Taylor, C. Jetter, L. Raju, J. Roberson, G. Ding, L. Wood, J. M. S. Sucre, B. W. Richmond, A. P. Serezani, W. J. McDonnell, S. B. Mallal, M. J. Bacchetta, J. E. Loyd, C. M. Shaver, L. B. Ware, R. Bremner, R. Walia, T. S. Blackwell, N. E. Banovich & J. A. Kropski (2020) Single-cell RNA sequencing reveals profibrotic roles of distinct epithelial and mesenchymal lineages in pulmonary fibrosis. *Sci Adv,* 6**,** eaba1972.

Harris, P., S. Sridhar, R. Peng, J. E. Phillips, R. G. Cohn, L. Burns, J. Woods, M. Ramanujam, M. Loubeau, G. Tyagi, J. Allard, M. Burczynski, P. Ravindran, D. Cheng, H. Bitter, J. S. Fine, C. M. Bauer & C. S. Stevenson (2013) Double-stranded RNA induces molecular and inflammatory signatures that are directly relevant to COPD. *Mucosal Immunol,* 6**,** 474-84.

Ismael, S. & T. Ishrat (2022) Compound 21, a Direct AT2R Agonist, Induces IL-10 and Inhibits Inflammation in Mice Following Traumatic Brain Injury. *Neuromolecular Med,* 24**,** 274-278.

Jabber, H., B. Mohammed & N. R. Hadi (2023) Investigating the renoprotective effect of C21 in male mice with sepsis via modulation of p-AKT/PI3K expression. *J Med Life,* 16**,** 203-209.

Kirsch-Volders, M. & M. Fenech (2021) Inflammatory cytokine storms severity may be fueled by interactions of micronuclei and RNA viruses such as COVID-19 virus SARS-CoV-2. A hypothesis. *Mutation Research-Reviews in Mutation Research,* 788.

Mei, D., W. S. D. Tan, W. Liao, C. K. M. Heng & W. S. F. Wong (2020) Activation of angiotensin II type-2 receptor protects against cigarette smoke-induced COPD. *Pharmacol Res,* 161**,** 105223.

Menk, M., J. A. Graw, C. von Haefen, H. Steinkraus, B. Lachmann, C. D. Spies & D. Schwaiberger (2018) Angiotensin II type 2 receptor agonist Compound 21 attenuates pulmonary inflammation in a model of acute lung injury. *J Inflamm Res,* 11**,** 169-178.

Murdaca, G., F. Paladin, A. Tonacci, S. Isola, A. Allegra & S. Gangemi (2021) The Potential Role of Cytokine Storm Pathway in the Clinical Course of Viral Respiratory Pandemic. *Biomedicines,* 9.

Nan, Y., C. Wu & Y. J. Zhang (2017) Interplay between Janus Kinase/Signal Transducer and Activator of Transcription Signaling Activated by Type I Interferons and Viral Antagonism. *Front Immunol,* 8**,** 1758.

Patel, S. N., N. Fatima, R. Ali & T. Hussain (2020) Emerging Role of Angiotensin AT2 Receptor in Anti-Inflammation: An Update. *Curr Pharm Des,* 26**,** 492-500.

Pfeffer, L. M. (2011) The role of nuclear factor κB in the interferon response. *J Interferon Cytokine Res,* 31**,** 553-9.

Sampson, A. K., J. C. Irvine, W. A. Shihata, D. Dragoljevic, N. Lumsden, O. Huet, T. Barnes, T. Unger, U. M. Steckelings, G. L. Jennings, R. E. Widdop & J. P. Chin-Dusting (2016) Compound 21, a selective agonist of angiotensin AT2 receptors, prevents endothelial inflammation and leukocyte adhesion in vitro and in vivo. *Br J Pharmacol,* 173**,** 729-40.

Schoggins, J. W. & C. M. Rice (2011) Interferon-stimulated genes and their antiviral effector functions. *Curr Opin Virol,* 1**,** 519-25.

Sikkema, L., C. Ramirez-Suastegui, D. C. Strobl, T. E. Gillett, L. Zappia, E. Madissoon, N. S. Markov, L. E. Zaragosi, Y. Ji, M. Ansari, M. J. Arguel, L. Apperloo, M. Banchero, C. Becavin, M. Berg, E. Chichelnitskiy, M. I. Chung, A. Collin, A. C. A. Gay, J. Gote-Schniering, B. Hooshiar Kashani, K. Inecik, M. Jain, T. S. Kapellos, T. M. Kole, S. Leroy, C. H. Mayr, A. J. Oliver, M. von Papen, L. Peter, C. J. Taylor, T. Walzthoeni, C. Xu, L. T. Bui, C. De Donno, L. Dony, A. Faiz, M. Guo, A. J. Gutierrez, L. Heumos, N. Huang, I. L. Ibarra, N. D. Jackson, P. Kadur Lakshminarasimha Murthy, M. Lotfollahi, T. Tabib, C. Talavera-Lopez, K. J. Travaglini, A. Wilbrey-Clark, K. B. Worlock, M. Yoshida, C. Lung Biological Network, M. van den Berge, Y. Bosse, T. J. Desai, O. Eickelberg, N. Kaminski, M. A. Krasnow, R. Lafyatis, M. Z. Nikolic, J. E. Powell, J. Rajagopal, M. Rojas, O. Rozenblatt-Rosen, M. A. Seibold, D. Sheppard, D. P. Shepherd, D. D. Sin, W. Timens, A. M. Tsankov, J. Whitsett, Y. Xu, N. E. Banovich, P. Barbry, T. E. Duong, C. S. Falk, K. B. Meyer, J. A. Kropski, D. Pe'er, H. B. Schiller, P. R. Tata, J. L. Schultze, S. A. Teichmann, A. V. Misharin, M. C. Nawijn, M. D. Luecken & F. J. Theis (2023) An integrated cell atlas of the lung in health and disease. *Nat Med,* 29**,** 1563-1577.

Steckelings, U. M. & C. Sumners (2020) Correcting the imbalanced protective RAS in COVID-19 with angiotensin AT2-receptor agonists. *Clin Sci (Lond),* 134**,** 2987-3006.

Steckelings, U. M., R. E. Widdop, E. D. Sturrock, L. Lubbe, T. Hussain, E. Kaschina, T. Unger, A. Hallberg, R. M. Carey & C. Sumners (2022) The Angiotensin AT(2) Receptor: From a Binding Site to a Novel Therapeutic Target. *Pharmacol Rev,* 74**,** 1051-1135.

Sumners, C., A. A. Peluso, A. H. Haugaard, J. B. Bertelsen & U. M. Steckelings (2019) Anti-fibrotic mechanisms of angiotensin AT. *Acta Physiol (Oxf),* 227**,** e13280.

Wang, D., X. Q. Chai, C. G. Magnussen, G. R. Zosky, S. H. Shu, X. Wei & S. S. Hu (2019) Renin-angiotensin-system, a potential pharmacological candidate, in acute respiratory distress syndrome during mechanical ventilation. *Pulm Pharmacol Ther,* 58**,** 101833.

Witherden, I. R. & T. D. Tetley (2001) Isolation and Culture of Human Alveolar Type II Pneumocytes. *Methods Mol Med,* 56**,** 137-46.

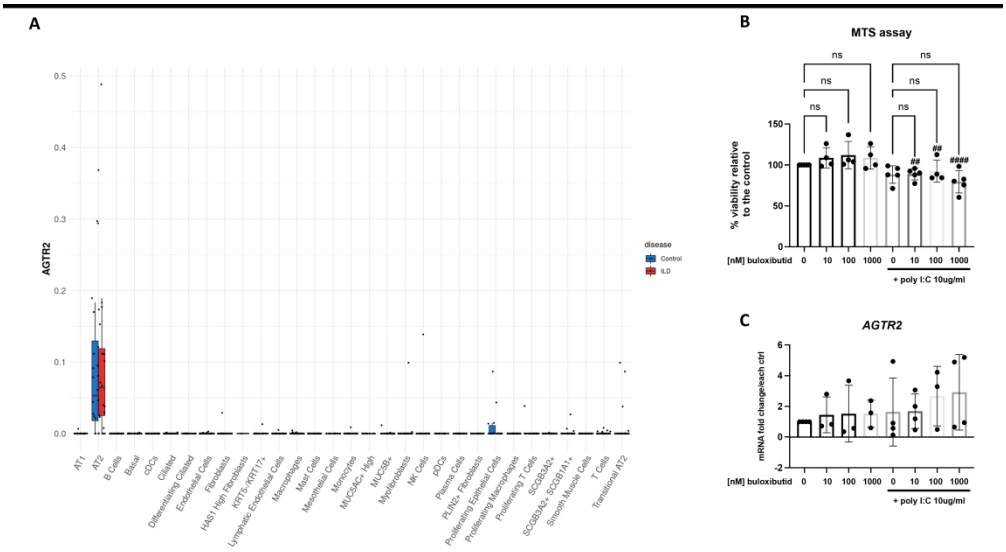

Fig.1: AT2 receptor gene (AGTR2) expression in lung cells and buloxibutid treatment (10–1000nM) of primary ATII cells in absence or presence of poly I:C. A) Banovich/Kropski dataset from the IPF atlas averaged per subject and braked by disease confirm the high expression of AT2 receptor in ATII cells in both control donors and ILD patients. B) MTS cell viability assay showed no significant effect of buloxibutid treatment on ATII cell viability (n=4/5). # – significance vs. equivalent buloxibutid-treated, poly-IC free culture. C) AT2 receptor gene expression is not modulated by buloxibutid compound treatment in absence or presence of poly I:C (n=3/4). Values are expressed as means of ± SD, of n=3-5 independent experiments, each performed using cells from a different donor. Samples were generated by pooling lysates from 3 wells per condition keeping donors separate and analysed in technical duplicate. Analysis: 2ways-ANOVA (p-value <0.01## and <0.0001####).

856x485mm (130 x 130 DPI)

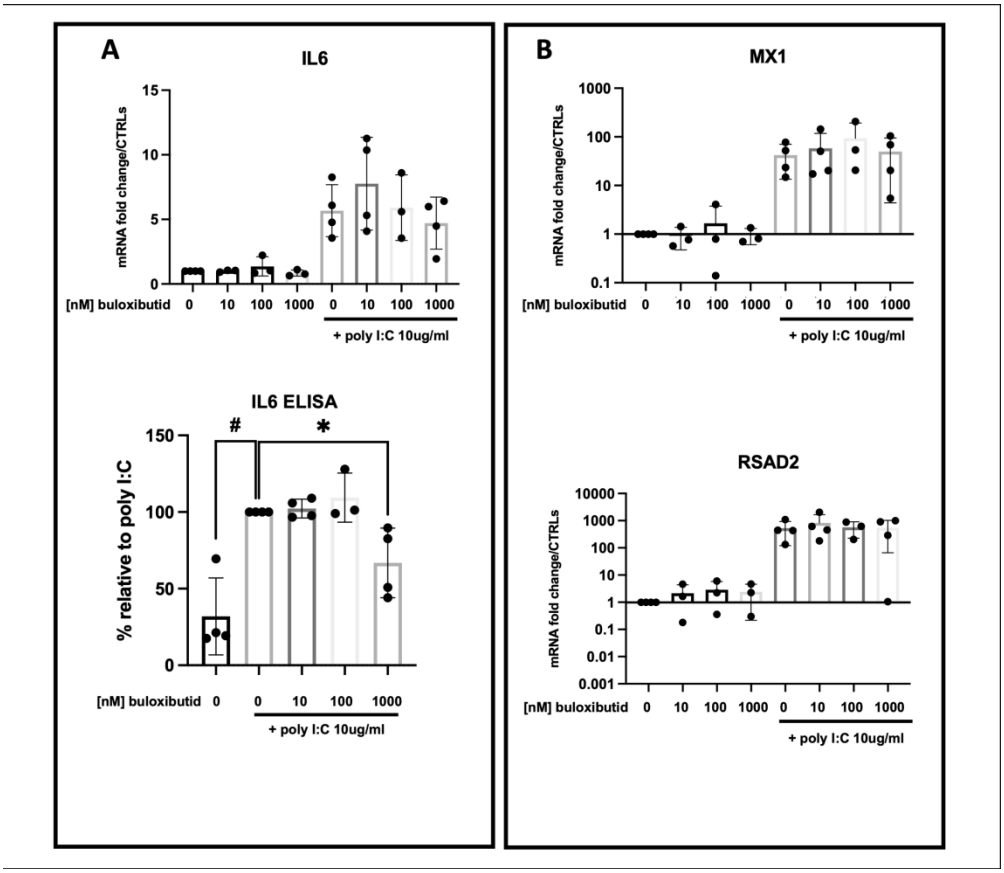

Fig.2: Expression of the inflammatory marker, IL6, and of anti-viral genes during buloxibutid treatment (10-1000nM) in absence or presence of poly I:C. A) Buloxibutid treatment shows a small, non-significant suppressive effect in IL6 gene expression induced by poly I:C, confirmed by a significant decrease in IL-6 protein release, measured by ELISA (bottom panel, Mann-Whitney p-value < 0.05 # ; oneway-ANOVA p-value < 0.05 *). B) Buloxibutid treatment does not affect induction of the anti-viral genes, MX1 or RSAD2, by poly I:C. Values are expressed as means of ± SD, of n=3-4 independent experiments, each performed using cells from a different donor. Samples were generated by pooling lysates or supernatants from 3 wells per condition keeping donors separate and analysed in technical duplicate. Analysis: 2ways-ANOVA (p-value < 0.05 *).

209x180mm (300 x 300 DPI)

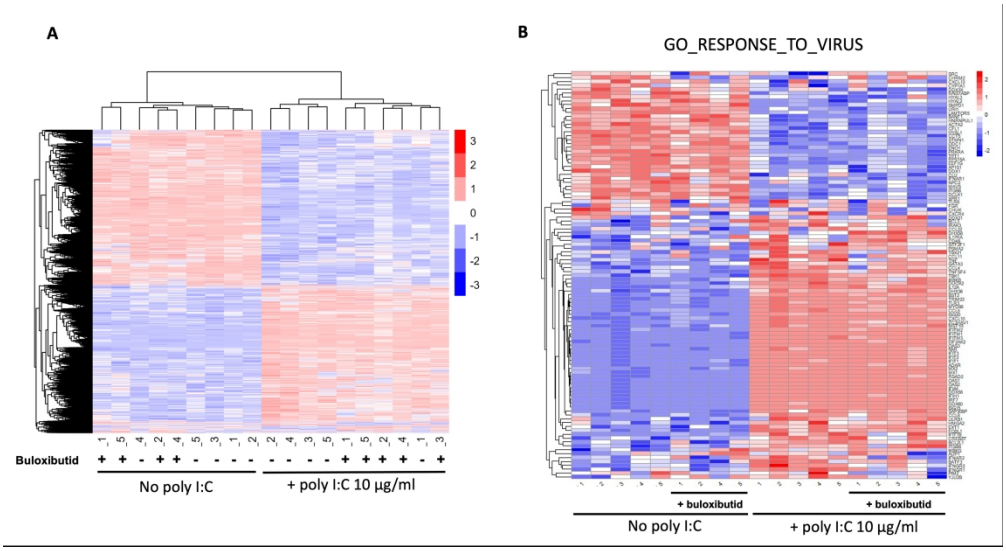

Fig.3: RNA sequencing of primary ATII cells treated with buloxibutid 1000nM in absence or presence of poly I:C. A) Heat map of all differentially expressed genes show a strong clustering mainly between conditions without or with poly I:C in absence or presence of buloxibutid 1000nM. B) Heatmap of GO_RESPONSE_TO_VIRUS genes show top differentially expressed genes clustering between conditions without or with poly I:C. n=4-5 independent experiments, each performed using cells from a different donor. Samples were generated by pooling lysates from 3 wells per condition keeping donors separate.

337x182mm (300 x 300 DPI)

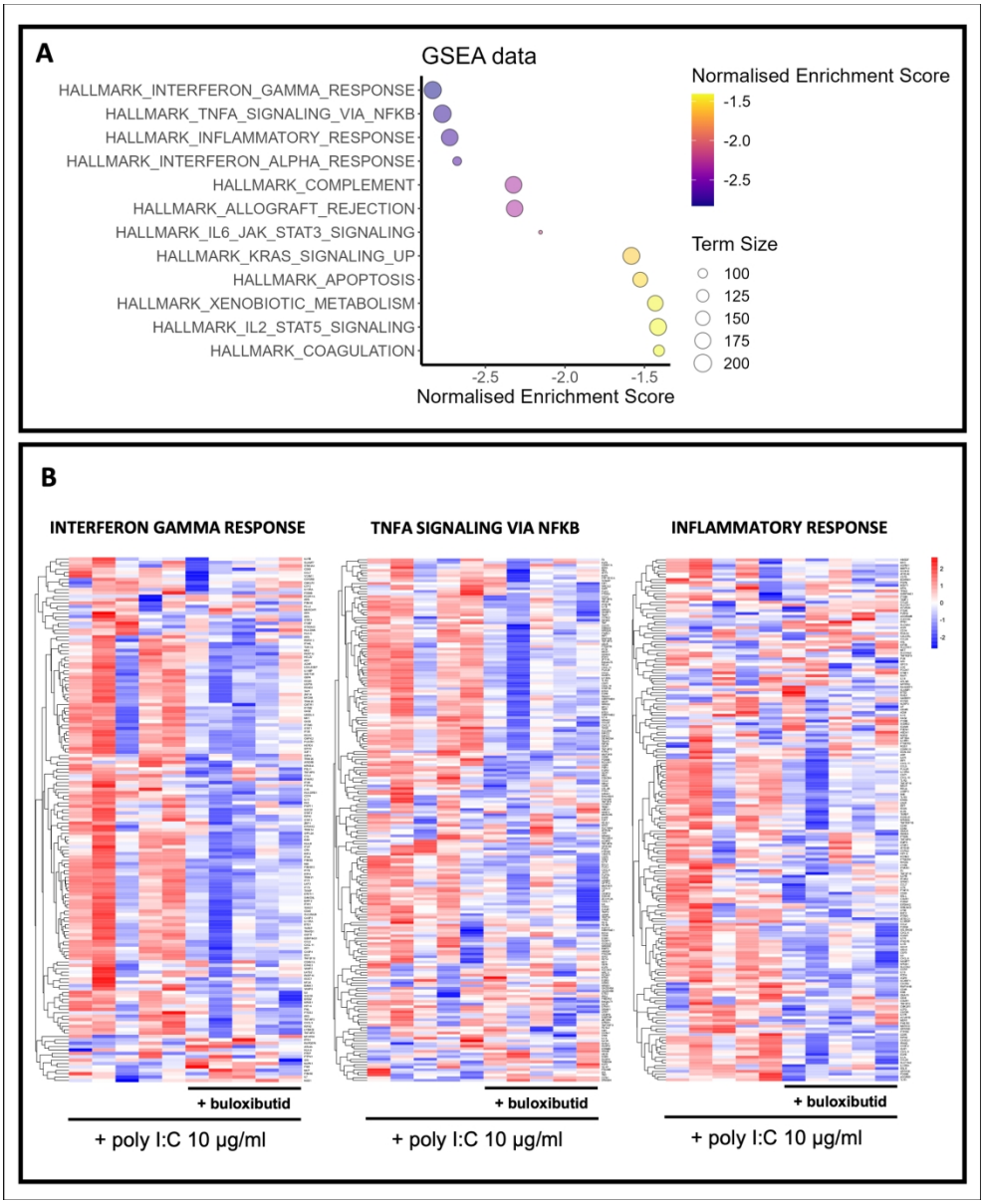

Fig.4: Gene set enrichment analysis (GSEA) of RNA sequencing datasets. A) GSEA analysis shows that mainly inflammation related pathways are significantly downregulated by buloxibutid 1000nM in presence of poly I:C compared to poly I:C alone (p-value < 0.05). B) Heat maps showing downregulation of the top 3 pathways of GSEA analysis by buloxibutid 1000nM in presence of poly I:C compared to poly I:C alone. n=5 independent experiments, each performed using cells from a different donor. Samples were generated by pooling lysates from 3 wells per condition keeping donors separate.

185x226mm (300 x 300 DPI)

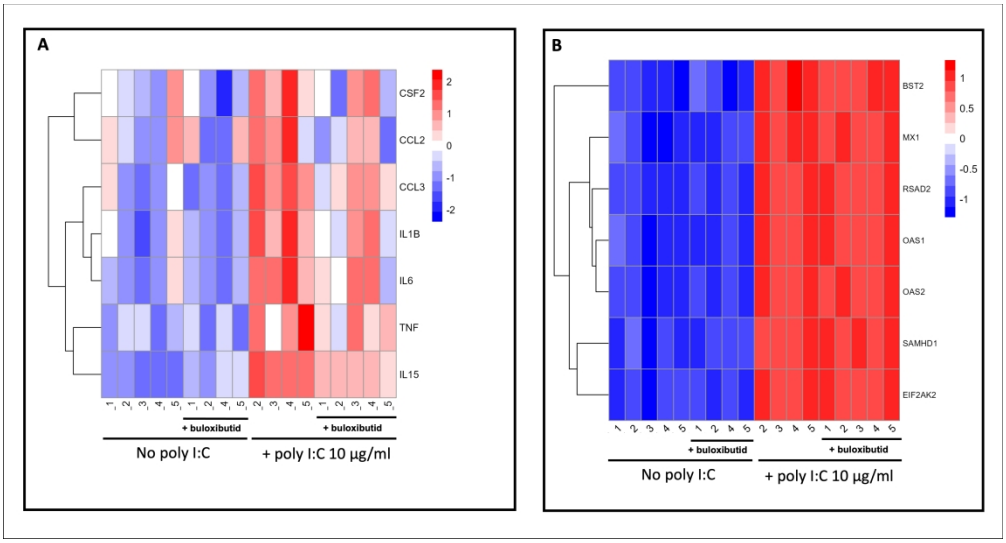

Fig.5: Mediators of the cytokine storm and antiviral transcripts during buloxibutid treatment. A) The Heatmap generated from RNA-sequencing shows that transcripts of the mediators of the cytokine storm are increased by poly I:C and down regulated by buloxibutid 1000nM treatment in presence of poly I:C. B) Antiviral genes induced by poly I:C treatment mimicked viral infection are not affected by buloxibutid compound 1000nM treatment. n=5 independent experiments, each performed using cells from a different donor. Samples were generated by pooling lysates from 3 wells per condition keeping donors separate.

336x179mm (330 x 330 DPI)

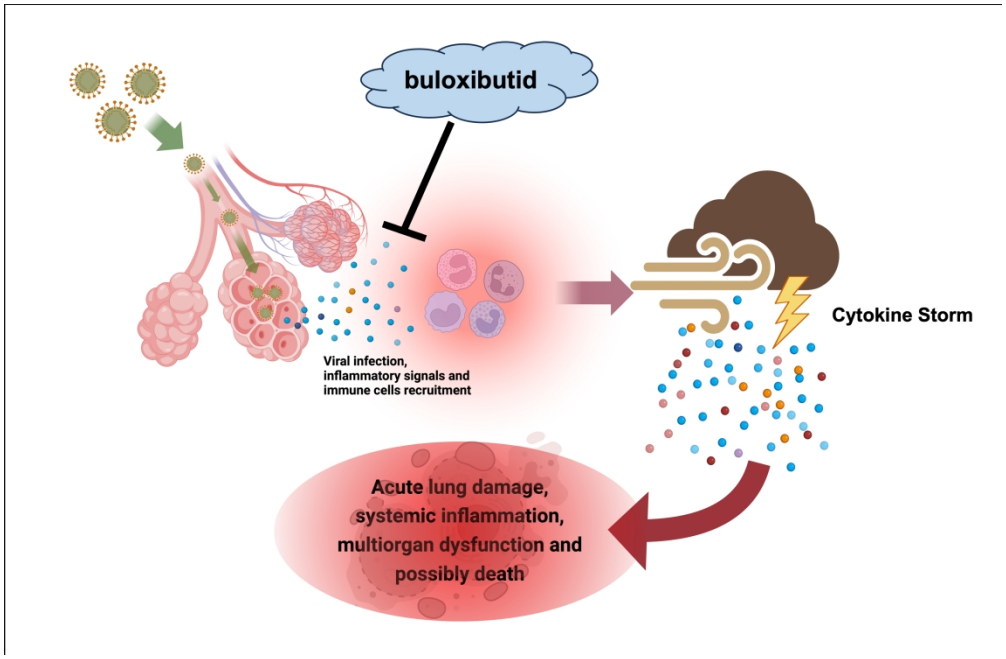

Fig.6: Graphical representation of role of buloxibutid in viral infection and inflammation. buloxibutid treatment during virus infection may help to reduce the cytokine storm by acting mainly on the alveolar cell mitigating the immune cell response.

256x166mm (330 x 330 DPI)

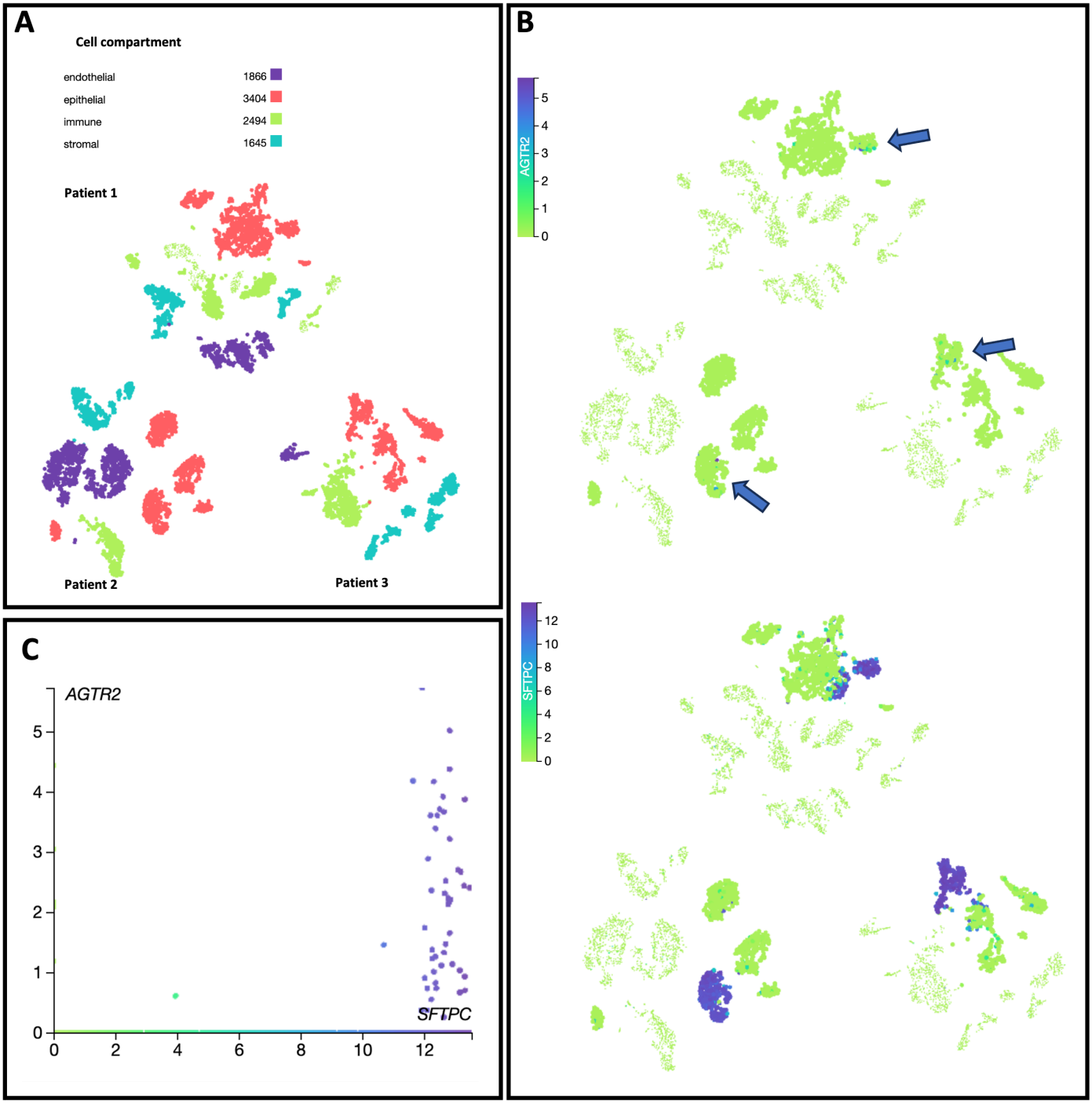

Supp. Fig.1: AGTR2 transcript is highly expressed in ATII cells in the lung. A) Krasnow human lung cell atlas from single-cell RNA sequencing cell compartment. B-C) AGTR2 is mainly expressed in the epithelial compartment and strongly correlates with SFTPC expression that is a specific marker of ATII cells.

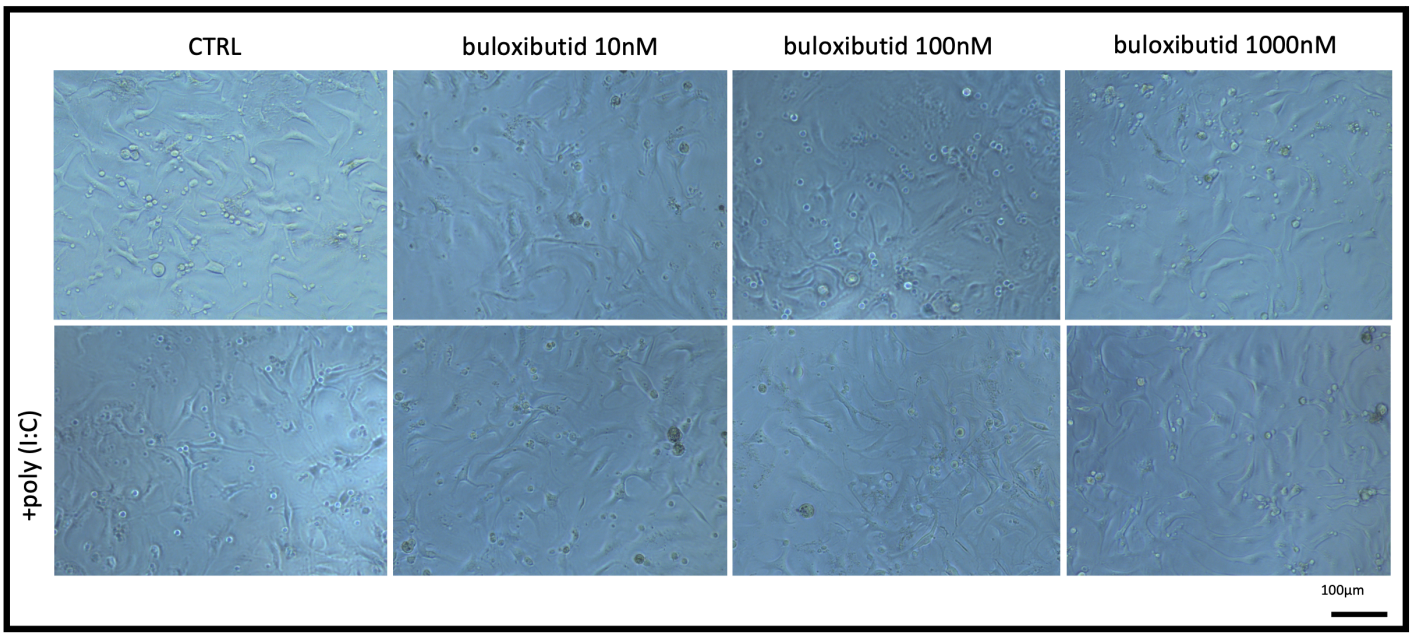

Supp. Fig.2: Buloxibutid (10-1000nM) treatment of primary ATII cells in absence or presence of poly I:C. shows no effects on ATII cell morphology and density.

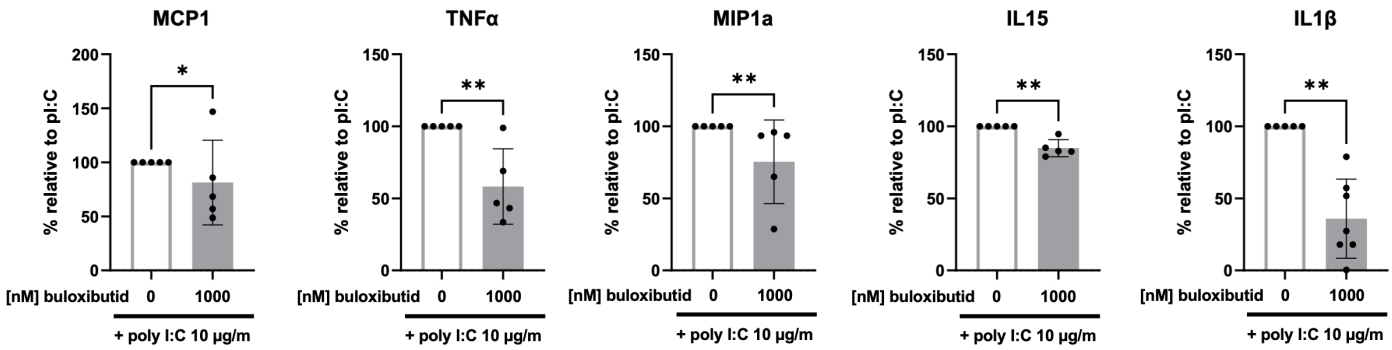

Supp. Fig.3: ATII cell protein release of the mediators of the cytokine storm is significantly down regulated by buloxibutid 1000nM treatment in presence of poly I:C treatment. Values are expressed as means of ± SD. Kolmogorov-Smirnov test (p-value < 0.05 * and p-value < 0.01 **).

GO_RESPONSE_TO_VIRUS

GENE SYMBOL	NCBI GENE ID	name
SRC	6714	SRC proto-oncogene, non-receptor tyrosine kinase
CHRM2	1129	cholinergic receptor muscarinic 2
CXCL12	6387	C-X-C motif chemokine ligand 12
CYP1A1	1543	cytochrome P450 family 1 subfamily A member 1
DDX3X	1654	DEAD-box helicase 3 X-linked
IVNS1ABP	10625	influenza virus NS1A binding protein
HYAL3	6677	sperm adhesion molecule 1
HYAL2	8692	hyaluronidase 2
SMPD1	6609	sphingomyelin phosphodiesterase 1
URI1	8725	URI1 prefoldin like chaperone
LAMTOR5	10542	late endosomal/lysosomal adaptor, MAPK and MTOR activator 5
BANF1	8815	barrier to autointegration nuclear assembly factor 1
HNRNPUL1	11100	heterogeneous nuclear ribonucleoprotein U like 1
ACTA2	59	actin alpha 2, smooth muscle
CFL1	6944	vacuolar protein sorting 72 homolog
HYAL1	6677	sperm adhesion molecule 1
CCT5	22948	chaperonin containing TCP1 subunit 5
STMN1	3925	stathmin 1
ODC1	89874	solute carrier family 25 member 21
ENO1	2023	enolase 1
PRKRA	8575	protein activator of interferon induced protein kinase EIF2AK2
TPT1	7178	tumor protein, translationally-controlled 1
RPS15A	6210	ribosomal protein S15a
EEF1G	1937	eukaryotic translation elongation factor 1 gamma
AP1S1	1174	adaptor related protein complex 1 subunit sigma 1
DDX1	1653	DEAD-box helicase 1
CLU	1191	clusterin
IFNAR1	3454	interferon alpha and beta receptor subunit 1
NPC2	10577	NPC intracellular cholesterol transporter 2
MAVS	57506	mitochondrial antiviral signaling protein
ITGB6	3694	integrin subunit beta 6
DCLK1	9201	doublecortin like kinase 1
XPR1	9213	xenotropic and polytropic retrovirus receptor 1
TLR8	51311	toll like receptor 8
FGR	2268	FGR proto-oncogene, Src family tyrosine kinase
CHUK	1147	component of inhibitor of nuclear factor kappa B kinase complex
CXCR4	7852	C-X-C motif chemokine receptor 4
DDX21	54606	DEAD-box helicase 56
BCL3	602	BCL3 transcription coactivator
IRAK3	11213	interleukin 1 receptor associated kinase 3
CCL22	6367	C-C motif chemokine ligand 22
DHX58	79132	DExH-box helicase 58
IL17RA	23765	interleukin 17 receptor A
CDK6	1021	cyclin dependent kinase 6
GTF2F1	2962	general transcription factor IIF subunit 1
PSMA2	5683	proteasome 20S subunit alpha 2
TBX21	30009	T-box transcription factor 21
CCL11	6356	C-C motif chemokine ligand 11
TNF	7124	tumor necrosis factor
GATA3	2625	GATA binding protein 3
CCL4	6351	C-C motif chemokine ligand 4
TNFSF4	7292	TNF superfamily member 4
TBK1	29110	TANK binding kinase 1
IKBKB	3551	inhibitor of nuclear factor kappa B kinase subunit beta
DUOX2	50506	dual oxidase 2
IL12A	3592	interleukin 12A
DHX36	170506	DEAH-box helicase 36
BST2	684	bone marrow stromal cell antigen 2
TRIM22	10346	tripartite motif containing 22
TLR3	7098	toll like receptor 3
MYD88	4615	MYD88 innate immune signal transduction adaptor
CCL5	6352	C-C motif chemokine ligand 5
ISG20	3669	interferon stimulated exonuclease gene 20
CXCL10	3627	C-X-C motif chemokine ligand 10
ZC3HAV1	56829	zinc finger CCCH-type containing, antiviral 1
MST1R	4486	macrophage stimulating 1 receptor
IFITM2	10581	interferon induced transmembrane protein 2
IFITM1	8519	interferon induced transmembrane protein 1
IFITM3	10410	interferon induced transmembrane protein 3
EIF2AK2	5610	eukaryotic translation initiation factor 2 alpha kinase 2
OAS3	4940	2'-5'-oligoadenylate synthetase 3
NMI	4641	myosin IC
IFIT3	3437	interferon induced protein with tetratricopeptide repeats 3
IFIT2	3433	interferon induced protein with tetratricopeptide repeats 2
IFIT1	3434	interferon induced protein with tetratricopeptide repeats 1
ADAR	103	adenosine deaminase RNA specific
MX2	4600	MX dynamin like GTPase 2
MX1	4599	MX dynamin like GTPase 1
RSAD2	91543	radical S-adenosyl methionine domain containing 2
OAS1	4938	2'-5'-oligoadenylate synthetase 1
OSA2	57492	AT-rich interaction domain 1B
IFI44	10561	interferon induced protein 44
DDX58	23586	RNA sensor RIG-I
IFIHI	64135	IFIH1 interferon induced with helicase C domain 1
IRF7	3665	interferon regulatory factor 7
DDX60	55601	DExD/H-box helicase 60
ISG15	9636	ISG15 ubiquitin like modifier
SAP30BP	29115	SAP30 binding protein
CCL8	6355	C-C motif chemokine ligand 8
LILRB1	10859	leukocyte immunoglobulin like receptor B1
HMGA2	8091	high mobility group AT-hook 2
EXT1	2131	exostosin glycosyltransferase 1
FOSL1	8061	FOS like 1, AP-1 transcription factor subunit
IFIT1B	439996	interferon induced protein with tetratricopeptide repeats 1B
CREBZF	58487	CREB/ATF bZIP transcription factor
BCL2L1	598	BCL2 like 1
ITGB8	3696	integrin subunit beta 8
IKBKG	8517	inhibitor of nuclear factor kappa B kinase regulatory subunit gamma
AUP1	550	AUP1 lipid droplet regulating VLDL assembly factor
IFNAR2	3455	interferon alpha and beta receptor subunit 2
BATF3	55509	basic leucine zipper ATF-like transcription factor 3
IFNGR2	3460	interferon gamma receptor 2
IFNGR1	3459	interferon gamma receptor 1
PIM2	11040	Pim-2 proto-oncogene, serine/threonine kinase
YJU2B	81576	YJU2 splicing factor homolog B

Supp. Table 1: Gene table of GO_RESPONSE_TO_VIRUS top differentially expressed genes

INTERFERON GAMMA RESPONSE

NAME	SYMBOL	RANK IN GENE LIST	RANK METRIC SCORE	RUNNING ES	CORE ENRICHMENT
row_0	DHX58	5	2.812493563	0.022039406	No
row_1	FPR1	659	1.071261883	-0.008064942	No
row_2	FCGR1A	847	0.98231405	-0.01132126	No
row_3	NUP93	1323	0.806831956	-0.033000473	No
row_4	NOD1	2540	0.537978709	-0.10062979	No
row_5	RAPGEF6	2708	0.509710491	-0.10645664	No
row_6	ARL4A	2729	0.506426573	-0.10361751	No
row_7	PIM1	3410	0.405891538	-0.1406023	No
row_8	IL7	3726	0.370510131	-0.15628578	No
row_9	KLRK1	4781	0.255617052	-0.21657844	No
row_10	METTL7B	4868	0.247142836	-0.21970093	No
row_11	UPP1	4917	0.242197067	-0.22061577	No
row_12	PFKP	6334	0.132888541	-0.30328798	No
row_13	FGL2	6715	0.109757349	-0.32488564	No
row_14	MVP	6748	0.107783154	-0.32592183	No
row_15	MARCHF1	7316	0.072829098	-0.35886994	No
row_16	MTHFD2	7376	0.06998869	-0.3618028	No
row_17	GZMA	7657	0.053877648	-0.3779312	No
row_18	ST3GAL5	9138	-0.024164269	-0.46525115	No
row_19	PSMB2	9646	-0.051518373	-0.49482074	No
row_20	GBP6	9770	-0.058492091	-0.5016292	No
row_21	ITGB7	9884	-0.064331405	-0.5077999	No
row_22	CDKN1A	9922	-0.067457199	-0.50945204	No
row_23	PSMB8	10249	-0.087390788	-0.52803427	No
row_24	PTPN1	10498	-0.103494667	-0.54187655	No
row_25	SRI	10519	-0.105065405	-0.54222476	No
row_26	IRF9	10539	-0.106833339	-0.54249984	No
row_27	SAMHD1	10715	-0.118334047	-0.5519078	No
row_28	PLA2G4A	10770	-0.121551633	-0.5541355	No
row_29	IRF8	10787	-0.122328751	-0.5541101	No
row_30	MX1	10857	-0.127217159	-0.55717975	No
row_31	RNF213	10962	-0.135506287	-0.5622531	No
row_32	VAMP5	11128	-0.147043467	-0.5708418	No
row_33	LATS2	11217	-0.153148264	-0.574829	No
row_34	OAS3	11536	-0.176062569	-0.592234	No
row_35	SECTM1	11576	-0.17845948	-0.5931229	No
row_36	EIF2AK2	11822	-0.198505223	-0.6060332	No
row_37	BST2	11881	-0.203923196	-0.60784334	No
row_38	OAS2	11949	-0.21026288	-0.6101352	No
row_39	EIF4E3	12082	-0.221719369	-0.6161796	No
row_40	PSMB9	12162	-0.228123814	-0.6190392	No
row_41	IFIT1	12192	-0.230105311	-0.6189266	No
row_42	IFI44L	12225	-0.233653829	-0.61896324	No
row_43	CXCL9	12241	-0.234772712	-0.6179857	No
row_44	IL18BP	12263	-0.236305773	-0.6173509	No
row_45	PTGS2	12301	-0.238701046	-0.61764306	No
row_46	IFI27	12497	-0.254707754	-0.6271506	No
row_47	APOL6	12509	-0.255321831	-0.62577343	No
row_48	ARID5B	12667	-0.269311428	-0.63291806	No
row_49	CMTR1	12696	-0.27212891	-0.6324126	No
row_50	EPSTI1	12788	-0.282074779	-0.63555336	No
row_51	MX2	12830	-0.286635786	-0.6357014	No
row_52	XAF1	12903	-0.293998778	-0.63762397	No
row_53	IFI30	12924	-0.295829922	-0.63645726	No
row_54	RSAD2	13004	-0.30449304	-0.63871044	No
row_55	MT2A	13125	-0.318330616	-0.643278	No
row_56	HLA-A	13230	-0.328852266	-0.64681596	Yes
row_57	HLA-G	13250	-0.330076903	-0.64531815	Yes
row_58	CSF2RB	13252	-0.330116421	-0.6427557	Yes
row_59	IRF5	13345	-0.34063983	-0.64549047	Yes
row_60	RBCK1	13351	-0.341596723	-0.6430734	Yes
row_61	IL4R	13382	-0.344388574	-0.6421123	Yes
row_62	CD86	13397	-0.345998466	-0.64019245	Yes
row_63	SERPING1	13429	-0.349055111	-0.6392535	Yes
row_64	ISG20	13432	-0.349526942	-0.636596	Yes
row_65	UBE2L6	13458	-0.351797044	-0.6352805	Yes
row_66	HLA-DQA1	13470	-0.353280872	-0.6331254	Yes
row_67	HLA-B	13488	-0.355876476	-0.63130444	Yes
row_68	STAT1	13500	-0.357912987	-0.62911254	Yes
row_69	CXCL11	13501	-0.358130306	-0.6262685	Yes
row_70	HIF1A	13527	-0.361531258	-0.6248757	Yes
row_71	TRIM25	13536	-0.362758607	-0.62246794	Yes
row_72	CXCL10	13557	-0.365175843	-0.62075055	Yes
row_73	IL2RB	13566	-0.366376609	-0.618314	Yes
row_74	HELZ2	13584	-0.368719757	-0.6163911	Yes
row_75	PSMA2	13670	-0.378201813	-0.6184137	Yes
row_76	PARP14	13697	-0.380375028	-0.61693037	Yes
row_77	IRF4	13719	-0.384550363	-0.6151182	Yes
row_78	ST8SIA4	13905	-0.411121219	-0.6227923	Yes
row_79	PNP	13945	-0.416422427	-0.6217914	Yes
row_80	ZBP1	14016	-0.427048594	-0.62253916	Yes
row_81	C1R	14085	-0.437128991	-0.62308854	Yes
row_82	DDX60	14172	-0.451118261	-0.62459123	Yes
row_83	CFB	14180	-0.452722549	-0.6214099	Yes
row_84	TRIM14	14195	-0.454235762	-0.6186304	Yes
row_85	TRIM26	14288	-0.467872888	-0.62035483	Yes
row_86	LGALS3BP	14431	-0.490724802	-0.6248542	Yes
row_87	IRF2	14441	-0.492017984	-0.62147903	Yes
row_88	CMKLR1	14453	-0.493866444	-0.6182075	Yes
row_89	VAMP8	14505	-0.501744866	-0.6172386	Yes
row_90	CD74	14516	-0.503022552	-0.61383516	Yes
row_91	HERC6	14540	-0.507386506	-0.6111658	Yes
row_92	STAT4	14542	-0.508006394	-0.60719067	Yes
row_93	PML	14544	-0.508409202	-0.60321236	Yes
row_94	IFIT2	14557	-0.509404123	-0.5998765	Yes
row_95	SLAMF7	14590	-0.51589334	-0.59767175	Yes
row_96	CCL5	14596	-0.516494691	-0.59386575	Yes
row_97	IL15RA	14606	-0.517648757	-0.5902871	Yes
row_98	CD38	14639	-0.523503184	-0.5880219	Yes
row_99	BANK1	14650	-0.527076423	-0.5844275	Yes
row_100	LY6E	14714	-0.537947893	-0.5838806	Yes
row_101	HLA-DMA	14794	-0.549838662	-0.58418536	Yes
row_102	STAT2	14903	-0.570400238	-0.5860416	Yes
row_103	NCOA3	14911	-0.571180522	-0.58191955	Yes
row_104	ZNFX1	14935	-0.574159026	-0.5787199	Yes
row_105	CMPK2	14966	-0.581629276	-0.57587487	Yes
row_106	PTPN6	14993	-0.587600112	-0.5727459	Yes
row_107	SOD2	15019	-0.591725528	-0.569525	Yes
row_108	ISG15	15030	-0.593333602	-0.5654044	Yes
row_109	IFIT3	15036	-0.594235003	-0.56098104	Yes
row_110	NLRC5	15045	-0.59562093	-0.556724	Yes
row_111	TAPBP	15084	-0.602952242	-0.5541827	Yes
row_112	PELI1	15101	-0.605130374	-0.5503232	Yes
row_113	LCP2	15145	-0.61355263	-0.5479933	Yes
row_114	PLSCR1	15281	-0.640206993	-0.5508917	Yes
row_115	IL10RA	15307	-0.646207213	-0.5472382	Yes
row_116	IFITM2	15367	-0.659097254	-0.5454927	Yes
row_117	AUTS2	15425	-0.673882961	-0.5435115	Yes
row_118	CFH	15478	-0.686697602	-0.5411329	Yes
row_119	STAT3	15483	-0.68844074	-0.5359023	Yes
row_120	PSMB10	15489	-0.689845622	-0.53071964	Yes
row_121	PNPT1	15508	-0.693703711	-0.526275	Yes
row_122	TRAFD1	15516	-0.695191741	-0.5211681	Yes
row_123	CASP1	15544	-0.701233566	-0.5171959	Yes
row_124	IFITM3	15569	-0.706519186	-0.51300424	Yes
row_125	PARP12	15616	-0.718521833	-0.51001817	Yes
row_126	C1S	15629	-0.722551405	-0.5049897	Yes
row_127	PSMA3	15638	-0.724852681	-0.4997064	Yes
row_128	TAP1	15661	-0.729404926	-0.49521476	Yes
row_129	VCAM1	15664	-0.730651736	-0.48953065	Yes
row_130	SSPN	15674	-0.73340255	-0.4842386	Yes
row_131	ADAR	15678	-0.733901739	-0.4785878	Yes
row_132	DDX58	15687	-0.737423301	-0.47320467	Yes
row_133	CD69	15708	-0.743967533	-0.46847916	Yes
row_134	MYD88	15743	-0.754565954	-0.46449727	Yes
row_135	PDE4B	15763	-0.759945691	-0.45958573	Yes
row_136	IDO1	15798	-0.76944989	-0.45548564	Yes
row_137	PSME1	15813	-0.774559855	-0.45016238	Yes
row_138	IRF7	15825	-0.777916849	-0.4446351	Yes
row_139	IFI35	15838	-0.782866836	-0.4391276	Yes
row_140	SAMD9L	15878	-0.796247959	-0.43511036	Yes
row_141	BATF2	15885	-0.79871875	-0.4291222	Yes
row_142	WARS1	15888	-0.802143693	-0.42287037	Yes
row_143	HLA-DRB1	15899	-0.805934846	-0.41706142	Yes
row_144	ICAM1	15909	-0.810719311	-0.41115537	Yes
row_145	IFI44	15920	-0.813309133	-0.40528786	Yes
row_146	CD274	15990	-0.837706208	-0.4027153	Yes
row_147	TNFAIP3	16001	-0.840808511	-0.3966294	Yes
row_148	CCL7	16015	-0.847289264	-0.39066947	Yes
row_149	B2M	16024	-0.850755334	-0.38438633	Yes
row_150	FAS	16085	-0.871020257	-0.381017	Yes
row_151	IFIH1	16154	-0.90075922	-0.37788457	Yes
row_152	GBP4	16178	-0.908811271	-0.37202734	Yes
row_153	CD40	16197	-0.919836164	-0.3657869	Yes
row_154	TOR1B	16232	-0.933071613	-0.36038744	Yes
row_155	PSME2	16245	-0.939611018	-0.3536352	Yes
row_156	CASP8	16247	-0.940875113	-0.3462225	Yes
row_157	USP18	16271	-0.955235183	-0.3399966	Yes
row_158	RIPK2	16293	-0.96371913	-0.33358505	Yes
row_159	SP110	16306	-0.97093159	-0.3265841	Yes
row_160	CCL2	16378	-1.007377028	-0.32278234	Yes
row_161	NFKBIA	16380	-1.008076906	-0.31483597	Yes
row_162	CIITA	16409	-1.020974636	-0.30838364	Yes
row_163	IRF1	16415	-1.025485873	-0.30053553	Yes
row_164	NFKB1	16449	-1.040415287	-0.2942245	Yes
row_165	TNFSF10	16467	-1.047913313	-0.28690782	Yes
row_166	TXNIP	16474	-1.050666094	-0.27891886	Yes
row_167	LYSMD2	16481	-1.053776503	-0.27090523	Yes
row_168	NMI	16529	-1.083244681	-0.26508185	Yes
row_169	IFNAR2	16571	-1.106220603	-0.25872126	Yes
row_170	TRIM21	16572	-1.106505513	-0.24993409	Yes
row_171	RNF31	16576	-1.109571576	-0.24129997	Yes
row_172	IL6	16588	-1.117834091	-0.23307326	Yes
row_173	BTG1	16610	-1.137616038	-0.22528075	Yes
row_174	CASP7	16621	-1.146034837	-0.21677096	Yes
row_175	ISOC1	16666	-1.182511568	-0.2099819	Yes
row_176	SOCS1	16701	-1.210018992	-0.2023831	Yes
row_177	NAMPT	16746	-1.242761612	-0.19511557	Yes
row_178	TNFAIP6	16768	-1.263355851	-0.1863245	Yes
row_179	OGFR	16821	-1.352745056	-0.17865661	Yes
row_180	CASP4	16846	-1.38225162	-0.16909873	Yes
row_181	RIPK1	16850	-1.389969707	-0.15823786	Yes
row_182	SPPL2A	16862	-1.409680128	-0.1476935	Yes
row_183	CASP3	16898	-1.477473617	-0.13802987	Yes
row_184	RTP4	16920	-1.507699728	-0.12729838	Yes
row_185	TNFAIP2	16925	-1.522113919	-0.11544723	Yes
row_186	BPGM	16941	-1.54917407	-0.104031615	Yes
row_187	SOCS3	16946	-1.563346624	-0.091853015	Yes
row_188	TDRD7	16948	-1.563658357	-0.07949455	Yes
row_189	LAP3	16968	-1.613212705	-0.0678069	Yes
row_190	GCH1	16985	-1.67679286	-0.055436935	Yes
row_191	PTPN2	16995	-1.710304379	-0.04238694	Yes
row_192	JAK2	17004	-1.747043252	-0.02898606	Yes
row_193	SLC25A28	17070	-2.128147602	-0.015929075	Yes
row_194	IL15	17085	-2.266460657	0.001241916	Yes

TNFA SIGNALING VIA NFKB

NAME	SYMBOL	RANK IN GENE LIST	RANK METRIC SCORE	RUNNING ES	CORE ENRICHMENT
row_0	DUSP4	19	2.417216301	0.017281447	No
row_1	DNAJB4	297	1.390185833	0.011482895	No
row_2	NR4A1	799	1.002622843	-0.0105156	No
row_3	HES1	1140	0.868199825	-0.02401494	No
row_4	EGR3	1322	0.806880474	-0.028576791	No
row_5	RHOB	1436	0.771483064	-0.029386165	No
row_6	CCN1	1470	0.763115287	-0.025527483	No
row_7	IRS2	1570	0.737502337	-0.025767533	No
row_8	GADD45B	1575	0.736353815	-0.020397354	No
row_9	SLC2A3	2117	0.614196599	-0.0477193	No
row_10	GADD45A	2518	0.542501688	-0.067247406	No
row_11	TUBB2A	3036	0.459060133	-0.09433107	No
row_12	KLF2	3428	0.404188246	-0.11438	No
row_13	NFAT5	4664	0.26582551	-0.18540262	No
row_14	BTG2	4701	0.262423635	-0.18553376	No
row_15	SIK1	5155	0.222957179	-0.21062975	No
row_16	SLC16A6	5369	0.204331025	-0.22167225	No
row_17	SGK1	5429	0.199984834	-0.2236392	No
row_18	PMEPA1	5646	0.18195124	-0.23502956	No
row_19	KLF9	5876	0.164498866	-0.24732171	No
row_20	AREG	5933	0.161556333	-0.24940382	No
row_21	ATP2B1	5938	0.161100164	-0.24841376	No
row_22	PDLIM5	6435	0.127035215	-0.27678344	No
row_23	F2RL1	6459	0.126006365	-0.2771844	No
row_24	GEM	6599	0.117573716	-0.28451058	No
row_25	BCL6	6784	0.10521204	-0.29459256	No
row_26	TNC	6885	0.098899499	-0.29975423	No
row_27	CCND1	6906	0.097957864	-0.30019128	No
row_28	ID2	7052	0.089626521	-0.30808517	No
row_29	IL6ST	7088	0.087449029	-0.30948946	No
row_30	JUN	7135	0.084711939	-0.31156522	No
row_31	KDM6B	7285	0.075570993	-0.31980273	No
row_32	NFIL3	7526	0.060441356	-0.33353782	No
row_33	BMP2	7581	0.057699233	-0.33629242	No
row_34	FJX1	7622	0.055673119	-0.3382344	No
row_35	IL18	8262	0.020922301	-0.37587008	No
row_36	NR4A2	8514	0.007706197	-0.39065734	No
row_37	ZBTB10	8533	0.006764367	-0.39167047	No
row_38	FOSL2	8680	-6.78E-04	-0.4003008	No
row_39	IER5	8755	-0.003749984	-0.4046491	No
row_40	ABCA1	8900	-0.010828603	-0.41308385	No
row_41	PLK2	9031	-0.017242255	-0.4206417	No
row_42	DUSP2	9205	-0.027594037	-0.43066403	No
row_43	ACKR3	9399	-0.037178431	-0.44179633	No
row_44	ETS2	9450	-0.039782323	-0.44445077	No
row_45	RCAN1	9498	-0.042879023	-0.4469042	No
row_46	TNFSF9	9503	-0.043017875	-0.44681326	No
row_47	SERPINE1	9539	-0.045043305	-0.44854042	No
row_48	PHLDA2	9562	-0.0461419	-0.4494903	No
row_49	PPP1R15A	9611	-0.049624853	-0.45195153	No
row_50	DUSP1	9886	-0.064524941	-0.46766654	No
row_51	CDKN1A	9922	-0.067457199	-0.46922305	No
row_52	CCNL1	10017	-0.072382428	-0.47423172	No
row_53	IER2	10098	-0.077886842	-0.47837046	No
row_54	SQSTM1	10141	-0.080234662	-0.4802437	No
row_55	TGIF1	10550	-0.107656918	-0.503556	No
row_56	CD44	10601	-0.1114484	-0.50566477	No
row_57	FOS	10651	-0.114550196	-0.5076907	No
row_58	FOSB	10711	-0.11799325	-0.510282	No
row_59	INHBA	10949	-0.134629697	-0.5232748	No
row_60	CEBPB	11062	-0.142374039	-0.52881515	No
row_61	F3	11233	-0.155194357	-0.5376885	No
row_62	REL	11405	-0.167298153	-0.5465288	No
row_63	PHLDA1	11940	-0.208538175	-0.5765255	No
row_64	MYC	12001	-0.21497488	-0.57843745	No
row_65	PTX3	12205	-0.23099272	-0.58868545	No
row_66	FOSL1	12249	-0.235216588	-0.58943784	No
row_67	PTGS2	12301	-0.238701046	-0.5906368	No
row_68	TIPARP	12372	-0.244772166	-0.5929133	No
row_69	SPSB1	12469	-0.251836687	-0.5966739	No
row_70	IL23A	12538	-0.257481962	-0.5987354	No
row_71	TRIB1	12554	-0.258686006	-0.5976529	No
row_72	TSC22D1	12583	-0.261601895	-0.5973171	No
row_73	KLF4	12622	-0.265213639	-0.5975453	No
row_74	ATF3	12935	-0.297291398	-0.61373556	No
row_75	FUT4	13074	-0.312803715	-0.61951613	No
row_76	TNFRSF9	13087	-0.3140122	-0.6178349	No
row_77	BCL3	13138	-0.319675654	-0.6183582	No
row_78	VEGFA	13224	-0.328263313	-0.6208862	No
row_79	B4GALT1	13229	-0.328678995	-0.61862016	No
row_80	CD80	13426	-0.348703295	-0.6275579	No
row_81	CXCL11	13501	-0.358130306	-0.6292079	No
row_82	BHLHE40	13533	-0.36222592	-0.6282834	No
row_83	CXCL10	13557	-0.365175843	-0.62686324	No
row_84	SPHK1	13560	-0.365589589	-0.62419784	No
row_85	TRIP10	13590	-0.36958766	-0.62309897	No
row_86	NFE2L2	13718	-0.384467542	-0.6276832	No
row_87	MARCKS	13839	-0.401325047	-0.63172513	No
row_88	SNN	13848	-0.402539462	-0.6291332	No
row_89	EIF1	13862	-0.404695004	-0.62682074	No
row_90	CCRL2	13918	-0.413292587	-0.6269269	No
row_91	PTGER4	13955	-0.418218136	-0.6258718	No
row_92	YRDC	13974	-0.420679837	-0.6237333	No
row_93	LAMB3	13987	-0.422561347	-0.6212256	No
row_94	CLCF1	14173	-0.451234281	-0.62873197	No
row_95	KLF10	14223	-0.459128171	-0.6281343	No
row_96	EFNA1	14274	-0.465904534	-0.62754416	No
row_97	PFKFB3	14452	-0.493840069	-0.63425297	No
row_98	IFIT2	14557	-0.509404123	-0.6365256	Yes
row_99	CCL5	14596	-0.516494691	-0.6348404	Yes
row_100	IL15RA	14606	-0.517648757	-0.6314312	Yes
row_101	EHD1	14618	-0.519556105	-0.62812585	Yes
row_102	PLPP3	14623	-0.520237744	-0.6244012	Yes
row_103	SMAD3	14626	-0.5206545	-0.62055516	Yes
row_104	HBEGF	14676	-0.531600058	-0.6194056	Yes
row_105	LDLR	14809	-0.552636445	-0.62300515	Yes
row_106	JAG1	14860	-0.560960948	-0.6216912	Yes
row_107	IER3	14872	-0.564230859	-0.6180456	Yes
row_108	PTPRE	14878	-0.565587521	-0.6140349	Yes
row_109	SOD2	15019	-0.591725528	-0.6178099	Yes
row_110	EDN1	15025	-0.592464209	-0.6135945	Yes
row_111	DRAM1	15039	-0.594878793	-0.60983384	Yes
row_112	PLAU	15074	-0.601263404	-0.6072667	Yes
row_113	SERPINB2	15108	-0.605879009	-0.60460526	Yes
row_114	KLF6	15197	-0.622549534	-0.60507	Yes
row_115	CXCL3	15237	-0.633175075	-0.6025556	Yes
row_116	LITAF	15240	-0.633741558	-0.5978484	Yes
row_117	CCL20	15273	-0.638515592	-0.5948793	Yes
row_118	KYNU	15597	-0.711541653	-0.608566	Yes
row_119	RELB	15619	-0.719807029	-0.6043273	Yes
row_120	CXCL1	15625	-0.721259892	-0.59913117	Yes
row_121	TAP1	15661	-0.729404926	-0.59564745	Yes
row_122	DDX58	15687	-0.737423301	-0.59151125	Yes
row_123	NFKBIE	15694	-0.739579797	-0.5862348	Yes
row_124	MAFF	15700	-0.740517199	-0.5808921	Yes
row_125	CXCL6	15702	-0.742177308	-0.5753001	Yes
row_126	CD69	15708	-0.743967533	-0.5699311	Yes
row_127	PDE4B	15763	-0.759945691	-0.56733865	Yes
row_128	SLC2A6	15783	-0.76522541	-0.56263584	Yes
row_129	PNRC1	15792	-0.767311156	-0.55726653	Yes
row_130	EGR1	15805	-0.771259367	-0.55210376	Yes
row_131	ZC3H12A	15850	-0.785433292	-0.5487257	Yes
row_132	PLAUR	15863	-0.789918542	-0.5434209	Yes
row_133	JUNB	15896	-0.804399312	-0.53918874	Yes
row_134	ICAM1	15909	-0.810719311	-0.5337255	Yes
row_135	CSF2	15978	-0.832214057	-0.5314108	Yes
row_136	IL7R	15979	-0.832727134	-0.52507025	Yes
row_137	GFPT2	15982	-0.833930254	-0.5188388	Yes
row_138	TNFAIP3	16001	-0.840808511	-0.51350135	Yes
row_139	SERPINB8	16031	-0.852505147	-0.5087254	Yes
row_140	BCL2A1	16059	-0.86141181	-0.50376344	Yes
row_141	PANX1	16076	-0.869087994	-0.49809232	Yes
row_142	CXCL2	16089	-0.872913837	-0.49215552	Yes
row_143	TLR2	16108	-0.879504204	-0.48652342	Yes
row_144	IFIH1	16154	-0.90075922	-0.48232645	Yes
row_145	LIF	16161	-0.902890623	-0.47580653	Yes
row_146	MAP2K3	16226	-0.930270493	-0.47250864	Yes
row_147	IL1B	16227	-0.93136704	-0.465417	Yes
row_148	PER1	16265	-0.951350212	-0.46036163	Yes
row_149	RIPK2	16293	-0.96371913	-0.45462063	Yes
row_150	MXD1	16361	-0.997790873	-0.4509861	Yes
row_151	TNFAIP8	16368	-1.001184821	-0.44371772	Yes
row_152	CCL2	16378	-1.007377028	-0.43657964	Yes
row_153	NFKBIA	16380	-1.008076906	-0.42896307	Yes
row_154	SAT1	16388	-1.009678125	-0.42168915	Yes
row_155	IL1A	16390	-1.010888815	-0.41405118	Yes
row_156	IRF1	16415	-1.025485873	-0.40766242	Yes
row_157	NFKB1	16449	-1.040415287	-0.4016923	Yes
row_158	B4GALT5	16465	-1.04743576	-0.3946041	Yes
row_159	BTG3	16490	-1.05941534	-0.38795698	Yes
row_160	DENND5A	16505	-1.067358732	-0.38065794	Yes
row_161	STAT5A	16514	-1.072957277	-0.37296137	Yes
row_162	PLEK	16531	-1.083437204	-0.3656582	Yes
row_163	TNIP1	16538	-1.085618615	-0.3577469	Yes
row_164	GPR183	16543	-1.088425517	-0.34969598	Yes
row_165	MCL1	16549	-1.092196226	-0.3416755	Yes
row_166	DUSP5	16550	-1.092561126	-0.33335647	Yes
row_167	RELA	16574	-1.109471798	-0.3262691	Yes
row_168	IL6	16588	-1.117834091	-0.31852654	Yes
row_169	CFLAR	16601	-1.126628876	-0.3106579	Yes
row_170	NFKB2	16605	-1.129356027	-0.30223617	Yes
row_171	BTG1	16610	-1.137616038	-0.2938107	Yes
row_172	OLR1	16615	-1.142597914	-0.28534725	Yes
row_173	NINJ1	16703	-1.214747667	-0.28124368	Yes
row_174	SDC4	16715	-1.221930385	-0.27259025	Yes
row_175	ZFP36	16716	-1.222496629	-0.26328188	Yes
row_176	NAMPT	16746	-1.242761612	-0.25553447	Yes
row_177	BIRC3	16757	-1.250611663	-0.2466035	Yes
row_178	TNFAIP6	16768	-1.263355851	-0.23757549	Yes
row_179	CCL4	16789	-1.297027349	-0.22888257	Yes
row_180	TNIP2	16813	-1.33784771	-0.22005627	Yes
row_181	NR4A3	16820	-1.3516711	-0.21011922	Yes
row_182	RNF19B	16824	-1.357024312	-0.19996396	Yes
row_183	TNF	16840	-1.370707273	-0.1904143	Yes
row_184	CSF1	16847	-1.383820534	-0.18023244	Yes
row_185	TANK	16866	-1.415804267	-0.17051683	Yes
row_186	EGR2	16876	-1.429410338	-0.1601653	Yes
row_187	CEBPD	16914	-1.500372887	-0.15092956	Yes
row_188	TNFAIP2	16925	-1.522113919	-0.13993129	Yes
row_189	MAP3K8	16927	-1.523493528	-0.12839021	Yes
row_190	IL12B	16939	-1.548800349	-0.11724791	Yes
row_191	SOCS3	16946	-1.563346624	-0.105699115	Yes
row_192	IFNGR2	16978	-1.652704	-0.094948605	Yes
row_193	GCH1	16985	-1.67679286	-0.082536	Yes
row_194	TRAF1	17000	-1.739671111	-0.0701178	Yes
row_195	G0S2	17010	-1.759135485	-0.057255663	Yes
row_196	MSC	17038	-1.876656651	-0.04456334	Yes
row_197	ICOSLG	17052	-1.964404821	-0.03037482	Yes
row_198	BIRC2	17071	-2.131563425	-0.015209253	Yes
row_199	CD83	17084	-2.261593819	0.001301278	Yes

INFLAMMATORY RESPONSE

NAME	SYMBOL	RANK IN GENE LIST	RANK METRIC SCORE	RUNNING ES	CORE ENRICHMENT
row_0	P2RY2	605	1.112942576	-0.02599243	No
row_1	FPR1	659	1.071261883	-0.01972827	No
row_2	CLEC5A	1368	0.789658546	-0.054643434	No
row_3	SLC4A4	1582	0.734343529	-0.06079019	No
row_4	KIF1B	1765	0.691433609	-0.06548128	No
row_5	STAB1	2319	0.574447274	-0.09312391	No
row_6	SLC7A1	2483	0.548074245	-0.09794959	No
row_7	RAF1	2641	0.519103527	-0.10267478	No
row_8	CD14	2760	0.502280772	-0.10524271	No
row_9	ITGB8	3084	0.452210337	-0.12036494	No
row_10	AHR	3649	0.37903139	-0.1503717	No
row_11	SGMS2	3653	0.378925562	-0.14722534	No
row_12	APLNR	4328	0.300891221	-0.18441828	No
row_13	ICAM4	4354	0.29828912	-0.18327935	No
row_14	BTG2	4701	0.262423635	-0.20142552	No
row_15	PSEN1	4752	0.257843196	-0.2021188	No
row_16	GP1BA	4901	0.24356994	-0.20872891	No
row_17	CALCRL	4958	0.239541829	-0.2099373	No
row_18	HAS2	5001	0.235283881	-0.21035568	No
row_19	ROS1	5314	0.208925307	-0.22696176	No
row_20	AXL	5511	0.192875296	-0.23685324	No
row_21	ATP2B1	5938	0.161100164	-0.260616	No
row_22	SLC31A1	6439	0.126935393	-0.28905168	No
row_23	ADORA2B	6442	0.126779392	-0.28805786	No
row_24	PVR	6473	0.125396967	-0.28873092	No
row_25	ACVR2A	6887	0.098896064	-0.312271	No
row_26	HPN	7278	0.076082148	-0.33465195	No
row_27	CCL24	7433	0.066463098	-0.3431701	No
row_28	PCDH7	7529	0.060308572	-0.34825543	No
row_29	OSM	7782	0.047850613	-0.36272848	No
row_30	GABBR1	7794	0.047216099	-0.3629644	No
row_31	CCL22	7841	0.045244373	-0.36528605	No
row_32	NPFFR2	8068	0.032054398	-0.37836108	No
row_33	C5AR1	8078	0.031537402	-0.37861633	No
row_34	IL18	8262	0.020922301	-0.3892478	No
row_35	ATP2A2	8493	0.00861425	-0.4027648	No
row_36	ITGA5	8615	0.002413692	-0.40989453	No
row_37	ABCA1	8900	-0.010828603	-0.4265834	No
row_38	PTGER2	8964	-0.013886819	-0.43018478	No
row_39	IL18R1	9322	-0.033194549	-0.4509917	No
row_40	TNFSF9	9503	-0.043017875	-0.46125203	No
row_41	SERPINE1	9539	-0.045043305	-0.46292537	No
row_42	SEMA4D	9566	-0.046413172	-0.46405482	No
row_43	DCBLD2	9594	-0.048250061	-0.46522725	No
row_44	TPBG	9600	-0.048709758	-0.4650955	No
row_45	CDKN1A	9922	-0.067457199	-0.4834743	No
row_46	TNFSF15	10397	-0.097158678	-0.51063466	No
row_47	LCK	10448	-0.100527771	-0.51270777	No
row_48	SRI	10519	-0.105065405	-0.5159231	No
row_49	ADM	10555	-0.108178779	-0.51704264	No
row_50	CXCR6	10559	-0.108306833	-0.51627	No
row_51	RGS16	10574	-0.109246224	-0.5161391	No
row_52	RGS1	10650	-0.114486717	-0.51956725	No
row_53	INHBA	10949	-0.134629697	-0.5359976	No
row_54	F3	11233	-0.155194357	-0.55136114	No
row_55	NOD2	11346	-0.163559869	-0.55654556	No
row_56	MET	11374	-0.165393665	-0.55669045	No
row_57	SELE	11384	-0.165970653	-0.5557666	No
row_58	EMP3	11500	-0.173782244	-0.56103855	No
row_59	ACVR1B	11690	-0.187129095	-0.5705668	No
row_60	ABI1	11704	-0.188654646	-0.5696803	No
row_61	KCNJ2	11767	-0.193959802	-0.57164305	No
row_62	EIF2AK2	11822	-0.198505223	-0.57309324	No
row_63	PDPN	11831	-0.199443325	-0.5718166	No
row_64	BST2	11881	-0.203923196	-0.5729238	No
row_65	MYC	12001	-0.21497488	-0.5780708	No
row_66	CXCL9	12241	-0.234772712	-0.59013605	No
row_67	FFAR2	12311	-0.239569992	-0.5921125	No
row_68	BDKRB1	12433	-0.24867256	-0.5970822	No
row_69	ITGB3	12585	-0.261774808	-0.6037099	No
row_70	IFITM1	12749	-0.278728038	-0.6108981	No
row_71	BEST1	12867	-0.289994806	-0.61526895	No
row_72	TNFRSF9	13087	-0.3140122	-0.6254571	No
row_73	TIMP1	13212	-0.326761603	-0.6299192	No
row_74	CD48	13350	-0.341318399	-0.6350218	Yes
row_75	LAMP3	13380	-0.344292402	-0.63371575	Yes
row_76	IL4R	13382	-0.344388574	-0.6307541	Yes
row_77	ADRM1	13471	-0.353440881	-0.63285464	Yes
row_78	CXCL11	13501	-0.358130306	-0.6314272	Yes
row_79	HIF1A	13527	-0.361531258	-0.62973356	Yes
row_80	CXCL10	13557	-0.365175843	-0.62824434	Yes
row_81	SPHK1	13560	-0.365589589	-0.62515587	Yes
row_82	IL2RB	13566	-0.366376609	-0.62223774	Yes
row_83	CD55	13680	-0.378762871	-0.6255936	Yes
row_84	KCNA3	13712	-0.383718163	-0.6240599	Yes
row_85	MSR1	13715	-0.384253442	-0.6208077	Yes
row_86	IFNAR1	13745	-0.388066649	-0.6191177	Yes
row_87	CCRL2	13918	-0.413292587	-0.6256575	Yes
row_88	LPAR1	13944	-0.416346788	-0.623483	Yes
row_89	PTGER4	13955	-0.418218136	-0.6204057	Yes
row_90	CYBB	13986	-0.422307521	-0.6184744	Yes
row_91	OSMR	14126	-0.443151802	-0.6228021	Yes
row_92	ATP2C1	14253	-0.463795155	-0.62618035	Yes
row_93	GNA15	14305	-0.471451283	-0.6250591	Yes
row_94	TNFRSF1B	14372	-0.479800671	-0.6247511	Yes
row_95	ADGRE1	14386	-0.483258545	-0.6212806	Yes
row_96	RASGRP1	14440	-0.492017627	-0.62009716	Yes
row_97	CMKLR1	14453	-0.493866444	-0.61647445	Yes
row_98	SELL	14554	-0.509339213	-0.6179167	Yes
row_99	CCL5	14596	-0.516494691	-0.61580944	Yes
row_100	SLC31A2	14604	-0.517424822	-0.6116846	Yes
row_101	IL15RA	14606	-0.517648757	-0.60720325	Yes
row_102	HBEGF	14676	-0.531600058	-0.6066182	Yes
row_103	LY6E	14714	-0.537947893	-0.60408634	Yes
row_104	PTGIR	14761	-0.544996858	-0.6020245	Yes
row_105	SCN1B	14789	-0.549350977	-0.5988016	Yes
row_106	LDLR	14809	-0.552636445	-0.59507716	Yes
row_107	NLRP3	14836	-0.556234717	-0.5917348	Yes
row_108	RHOG	14850	-0.557733178	-0.587611	Yes
row_109	SLAMF1	14857	-0.560833037	-0.5830464	Yes
row_110	PTPRE	14878	-0.565587521	-0.5792674	Yes
row_111	CD70	14881	-0.565961421	-0.5744214	Yes
row_112	GPC3	14999	-0.588378906	-0.57617503	Yes
row_113	EDN1	15025	-0.592464209	-0.57245576	Yes
row_114	P2RX4	15060	-0.597848475	-0.5692212	Yes
row_115	TAPBP	15084	-0.602952242	-0.5652918	Yes
row_116	IL1R1	15128	-0.610241354	-0.5624804	Yes
row_117	LCP2	15145	-0.61355263	-0.5580443	Yes
row_118	KLF6	15197	-0.622549534	-0.5555978	Yes
row_119	CCL20	15273	-0.638515592	-0.55442953	Yes
row_120	IL10RA	15307	-0.646207213	-0.5507117	Yes
row_121	HRH1	15346	-0.653422058	-0.547226	Yes
row_122	MMP14	15444	-0.680049241	-0.5469936	Yes
row_123	MARCO	15506	-0.693301976	-0.54451746	Yes
row_124	CD82	15534	-0.698675394	-0.5399848	Yes
row_125	GNAI3	15568	-0.706324458	-0.53573966	Yes
row_126	RNF144B	15571	-0.707458198	-0.52965254	Yes
row_127	TLR3	15591	-0.710584342	-0.5245426	Yes
row_128	EREG	15599	-0.713270009	-0.5187	Yes
row_129	CSF3	15672	-0.732647836	-0.51652884	Yes
row_130	PIK3R5	15675	-0.733457267	-0.5102136	Yes
row_131	CXCL6	15702	-0.742177308	-0.5052403	Yes
row_132	CD69	15708	-0.743967533	-0.49901026	Yes
row_133	PDE4B	15763	-0.759945691	-0.49553585	Yes
row_134	IRF7	15825	-0.777916849	-0.49231747	Yes
row_135	CXCL8	15852	-0.785575569	-0.4869635	Yes
row_136	PLAUR	15863	-0.789918542	-0.48062587	Yes
row_137	LYN	15882	-0.79768151	-0.47469294	Yes
row_138	ICAM1	15909	-0.810719311	-0.46911842	Yes
row_139	IL7R	15979	-0.832727134	-0.4658921	Yes
row_140	CCL7	16015	-0.847289264	-0.4605287	Yes
row_141	EBI3	16020	-0.84941119	-0.45331463	Yes
row_142	TLR2	16108	-0.879504204	-0.4507418	Yes
row_143	LIF	16161	-0.902890623	-0.44589537	Yes
row_144	CD40	16197	-0.919836164	-0.43989563	Yes
row_145	IL1B	16227	-0.93136704	-0.43344018	Yes
row_146	RIPK2	16293	-0.96371913	-0.42882848	Yes
row_147	IL10	16298	-0.967557073	-0.42057815	Yes
row_148	PTAFR	16319	-0.974483311	-0.41321263	Yes
row_149	MXD1	16361	-0.997790873	-0.40688372	Yes
row_150	CCL2	16378	-1.007377028	-0.39899328	Yes
row_151	NFKBIA	16380	-1.008076906	-0.3902102	Yes
row_152	IL1A	16390	-1.010888815	-0.38187528	Yes
row_153	IRF1	16415	-1.025485873	-0.3742988	Yes
row_154	NFKB1	16449	-1.040415287	-0.36712325	Yes
row_155	TNFSF10	16467	-1.047913313	-0.35893634	Yes
row_156	NMI	16529	-1.083244681	-0.35303986	Yes
row_157	FZD5	16532	-1.083474398	-0.34365457	Yes
row_158	GPR183	16543	-1.088425517	-0.33469865	Yes
row_159	GPR132	16561	-1.097692013	-0.32607514	Yes
row_160	RELA	16574	-1.109471798	-0.31705278	Yes
row_161	SELENOS	16578	-1.11089313	-0.3074861	Yes
row_162	IL6	16588	-1.117834091	-0.29821312	Yes
row_163	AQP9	16594	-1.123367667	-0.28865522	Yes
row_164	C3AR1	16613	-1.139947414	-0.27972016	Yes
row_165	OLR1	16615	-1.142597914	-0.26975718	Yes
row_166	SCARF1	16644	-1.162762165	-0.26121297	Yes
row_167	SLC11A2	16686	-1.196379423	-0.2531422	Yes
row_168	NAMPT	16746	-1.242761612	-0.24572836	Yes
row_169	TNFAIP6	16768	-1.263355851	-0.23588814	Yes
row_170	TLR1	16774	-1.269525051	-0.22504824	Yes
row_171	SLC7A2	16797	-1.310408592	-0.2148544	Yes
row_172	CSF1	16847	-1.383820534	-0.2056123	Yes
row_173	IL18RAP	16907	-1.492377043	-0.19600901	Yes
row_174	RTP4	16920	-1.507699728	-0.18349369	Yes
row_175	CX3CL1	16922	-1.515523314	-0.17025967	Yes
row_176	IL12B	16939	-1.548800349	-0.15762025	Yes
row_177	IFNGR2	16978	-1.652704	-0.1453696	Yes
row_178	GCH1	16985	-1.67679286	-0.13101654	Yes
row_179	CSF3R	17002	-1.742615461	-0.11667709	Yes
row_180	IRAK2	17019	-1.788577199	-0.10193451	Yes
row_181	CHST2	17023	-1.815775156	-0.08618509	Yes
row_182	ICOSLG	17052	-1.964404821	-0.07060944	Yes
row_183	IL15	17085	-2.266460657	-0.05262077	Yes
row_184	P2RX7	17099	-2.579213381	-0.03076598	Yes
row_185	CCR7	17105	-3.548093913	5.95E-05	Yes

Supp. Table 2: Data tables of GSEA hallmark interferon gamma response, hallmark TNFA signaling via NFKB and hallmark inflammatory response.